Ecosystem response to weather extremes and impact on atmospheric composition

A case study of the 2018 summer heatwave

Master's thesis

Sara Bengtsdotter

LUND UNIVERSITY

Supervisor: Pontus Roldin
Deputy supervisor: Lars Nieradzik
Examiner: Erik Swietlicki

Division of Combustion Physics
Lund University
Lund, Sweden
May, 2024

Abstract

Extreme weather events, such as heatwaves and droughts, are predicted to increase due to global warming, significantly impacting forest ecosystems. These ecosystems play a crucial role in the climate system through carbon sequestration and the emission of Biogenic Volatile Organic Compounds (BVOCs), which can form Secondary Organic Aerosols (SOAs) and thus have a cooling effect on the climate. In this study, BVOC emission data from the dynamic vegetation model LPJ-GUESS and the BVOC emission model MEGAN is used to investigate the response of a boreal forest ecosystem during the 2018 summer heatwave in northern Europe. Furthermore, the impact on atmospheric composition is examined by using these BVOC emission datasets as input in the atmospheric model ADCHEM, set up as a 1D-column model along pre-calculated air mass trajectories. Both datasets were tested for both 2017 and 2018, and compared with observed concentrations of isoprene, total monoterpenes, NO_x and O_3, as well as particle number size distribution from the SMEAR II station in Hyytiälä, southern Finland. The results indicate that most model setups underestimated isoprene and monoterpene concentrations, except for LPJ-GUESS, which significantly overestimated isoprene concentrations for both years. Further, while the observed increase in particle volume during May and July 2018 is somewhat captured by the model setups, the particle number concentrations are underestimated. Models show a depletion of OH during May and July 2018, which may be an effect of the increased BVOC concentrations. Further studies on the 2018 drought should include other measurement stations in northern European boreal forests.

Ökade utsläpp från vegetation under torka skapar osäkerhet i modellering av framtida klimat!

Extremväder, såsom torkan 2018, förväntas öka i framtiden på grund av den pågående globala uppvärmningen. Detta kommer bland annat påverka världens skogar, vilka är viktiga i klimatsystemet, framför allt på grund av deras förmåga att binda koldioxid, men även deras utsläpp av biogena volatila organiska kolväten. Skogarnas förutsättningar att bidra till klimatsystemet på detta sätt kan dock ändras under extremväder - alltså är det viktigt att de modeller som används för att förutspå framtida klimat kan representera hur dessa extremväder påverkar skogarna.

Den som varit ute i Sveriges skogar har säkerligen lagt märke till att skogen doftar. Denna doft kommer från små molekyler som släpps ut av träden, kallade biogena volatila organiska kolväten (med den engelska förkortningen BVOC). Dessa används av alla växter för till exempel kommunikation mellan individer eller försvar mot attackerande insekter. Men BVOCer spelar också stor roll för klimatsystemet, eftersom de, genom komplexa reaktioner i atmosfären, kan bidra till tillväxt av aerosolpartiklar - små fasta eller flytande partiklar i atmosfären. Aerosolpartiklar ökar reflektionen av solljus från jorden och har därmed en kylande effekt. Generellt sett ökar utsläpp av BVOCer när träden är stressade, vilket de exempelvis blir under torka. Dessa ökade utsläpp kan alltså ha en kylande effekt, men också andra konsekvenser såsom bildande av marknära ozon - vilket är både en växthusgas som bidrar till global uppvärmning, och farlig för människor och träd.

I detta examensarbete undersöker jag hur utsläppen av BVOCer från nordiska skogar påverkades av torkan 2018, och hur väl detta representeras i vegetations- och atmosfärsmodeller. Eftersom modeller används för att förutspå framtidens klimat är det viktigt att de också representerar de klimatåterkopplingsmekanismer som involverar skogen. Annars kan vi få en felaktig bild av hur vårt framtida klimat kommer se ut, och det blir svårt att både förbereda sig för eller försöka motverka det. Två modeller som beräknar utsläpp av BVOCer, och en atmosfärsmodell, som beskriver hur dessa ämnen reagerar i atmosfären, undersöktes och utvärderades mot en mätstation i södra Finland. Både modeller och mätvärden visar att utsläpp av BVOCer ökade under 2018 och att detta även påverkade tillväxten av aerosolpartiklar, framför allt i Maj och Juli, som var de varmaste månaderna under 2018. Det visade sig dock att utsläppen generellt sett underskattades i båda modellerna, även om en typ av BVOC överskattades stort i en av modellerna. Varken över- eller underskattning var unik för året 2018, men blev mer dramatisk. Även om modellerna lyckades fånga en viss tillväxt av aerosolpartiklar under de månader med höga utsläpp var det totala antalet partiklar underskattad, vilket skulle kunna bero på att den underskattar antingen utsläpp av partiklar, eller nypartikelbildning - alltså att partiklar bildas i atmosfären. Dessa resultat kan förhoppningsvis bli en grund för vidare undersökningar om hur olika modeller representerar påverkan av extremväder, och därigenom leda till bättre uppskattningar om vårt framtida klimat.

Acknowledgements

This thesis would not have been possible without the input and encouragement from several people. First of all, I would like to extend my gratitude to my supervisor, Pontus Roldin at the Department of Physics, not only for supervising my thesis - but for encouraging and guiding me throughout my atmospheric modelling journey. Without your initial support, I would probably not have chosen to pursue this in my studies, nor my thesis. Further, I would like to thank Lars Nieradzik and Paul Miller at the Department of Physical Geography and Ecosystem Science. Lars for your work as deputy supervisor and for running the LPJ-GUESS simulations used in this thesis, and Paul, for your involvement in formulation and early stages of the project, despite not having a formal supervising role. I also want to thank Erik Swietlicki at the Department of Physics for your work as examiner for this project, and Henrik Palme for your work as opponent. Thank you also to Robin Wollesen de Jonge for your input on the report, as well as the rest of the atmospheric modelling group for making me feel included in your work and for listening and commenting on my problems during the course of this thesis.

Finally, thanks to my friends and family for your endless support during this time, and throughout my life. You have listened to me complain and celebrated my progress, kept me company while studying and provided me with much needed breaks. Thank you especially to my brother, Erik Nyström, who aside from this, also has made the illustrations used in some of the figures in this thesis.

Acronyms

ADCHEM Aerosol Dynamics and gas phase CHEMistry model. 3, 11

BA burnt area. 6

BVOC Biogenic Volatile Organic Compunds. 3, 6

CAMS Copernicus Atmosphere Monitoring Service. 3, 11

CCN Cloud Condensation Nuclei. 3, 8

CDNC cloud droplet number concentration. 8

DVM Dynamic vegetation model. 3, 11

HOM Highly Oxygenated organic Molecules. 7

LPJ-GUESS Lund-Potsdam-Jena General Ecosystem Simulator. 3, 11

MEGAN Model of Emissions of Gases and Aerosols from Nature. 3, 11

NPF New particle formation. 9

PFTs Plant Functional Types. 12

RF Radiative Forcing. 3

SOA Secondary organic aerosol. 10

Contents

1 Introduction

Forests play a crucial role in the climate system, primarily through sequestration of carbon dioxide via photosynthesis, which has a cooling effect on the climate (Šimpraga et al., 2019). A small fraction of this carbon is however re-emitted back into the atmosphere in the form of Biogenic Volatile Organic Compunds (BVOC). These small organic compounds are responsible for the scent associated with pine forests, but also play a key role in the formation and growth of aerosol particles - small solid or liquid particles suspended in air.

Aerosol particles and their interaction with clouds constitute one of the largest uncertainties in climate predictions (IPCC, 2021). Overall, they have a net cooling effect on the climate, both directly and indirectly. The direct effect originates from the fact that aerosol particles scatter incoming solar radiation, affecting the amount of radiation that reaches the earth surface and hence, cool the earth. The indirect effect is attributed to the fact that certain aerosol particles have the ability to act as "cloud seeds" or Cloud Condensation Nuclei (CCN), and aid in cloud formation, increasing cloud coverage and further the reflectivity of clouds. Water droplets in clouds reflect solar radiation back to space, meaning this also continuities a cooling effect on the climate. Typically, CCN particles are larger than 50 nm in diameter and water soluble (Berg Malmborg, 2014).

BVOC have a short atmospheric lifetime (minutes to days) as they are rapidly oxidized by atmospheric oxidants such as ozone (O_3), hydroxyl (OH) and nitrate (NO_3) radicals, and thus affect the oxidizing capacity of the atmosphere. Some studies suggest that lowered concentrations of OH radicals, because they react with BVOC, might prolong the atmospheric lifetime of methane, a strong greenhouse gas (Boy et al., 2022), of which OH is the main sink. Further, oxidation of BVOC in the presence of Nitrogen oxides (NO_x) leads to formation of tropospheric ozone, which is both a greenhouse gas and act as stresses for trees. In this way, BVOC might also have a warming effect on the climate. Figure 1 provides an overview of some of the mentioned processes.

With increasing global temperatures, extreme weather events such as droughts are expected to increase in frequency and/or severity (Wilcke et al., 2020). One such event, attributed to climate change, was the 2018 summer heatwave experienced by Europe, which caused drought and wildfire events throughout northern Europe. High temperatures, water scarcity and wildfires are stresses on vegetation that affect their ability to produce and emit BVOCs. Knowing how extreme events such as these affect the forest climate impact is an important part in evaluating the climate impact of forest ecosystems. Therefore, the focus of this thesis is to quantify the impact of the 2018 heatwave on boreal forests in northern Europe, as well as the impact on atmospheric composition. Two different datasets of BVOC emissions was used to model the atmospheric processes associated with BVOC emissions in the *Aerosol Dynamics and gas phase CHEMistry model* (ADCHEM). One of these datasets was generated with the Dynamic vegetation model (DVM) *Lund-Potsdam-Jena General Ecosystem Simulator* (LPJ-GUESS), and the other using *Model of Emissions of Gases and Aerosols from Nature* (MEGAN), accessed through Copernicus Atmosphere Monitoring Service (CAMS).

Understanding the climate impact of forest ecosystems, and how this impact might be affected by global warming, is important not only to improve climate predictions, but to guide forestry. At a larger scale, this is done in the ongoing EU project CLIMB-FOREST (CLImate Mitigation and Bioeconomy pathways for sustainable FORESTry), launched in 2022 in order to provide a comprehensive overview of European forests and forestry, to guide policy and practise. Part of the project is process modelling of emissions and effects on atmospheric chemistry and Radiative Forcing (RF) of Biogenic Volatile Organic Compunds (BVOC), in order to quantify climate impact of forest ecosystems. Therefore, part of the current thesis also serves as an evaluation of the ability of the employed models to reproduce the effects of the extreme weather experienced in 2018.

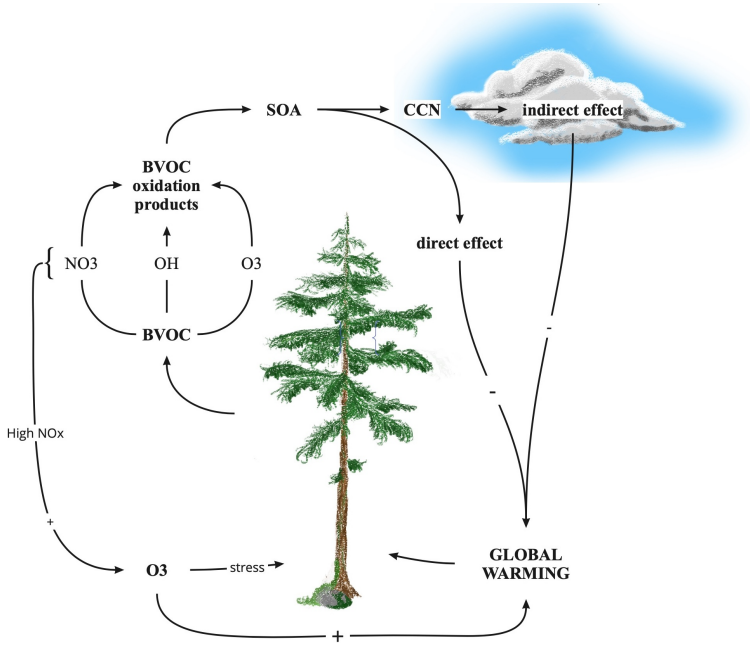

Figure 1: The figure provides an overview of some of the atmospheric atmospheric processes associated with BVOC and their effect on global warming. BVOC are emitted from trees and oxidized in the atmosphere by NO_3, OH and O_3 radicals. BVOC oxidation products can condense onto particles in the atmosphere and form SOA. These particles can lead to CNN activation (indirect effect) or scattering of solar radiation (direct effect), which has a cooling effect on the climate (indicated by "-" in the figure). However, oxidation of BVOC in the precense of NO_x can lead to net formation of O_3, which is a strong greenhouse gas and can facilitate global warming (indicated by "+" in the figure). Further, elevated O_3-levels, global warming and associated processes act as stresses on trees, which affect their emission of BVOC. (Illustrations by Erik Nyström, 2024)

1.1 Aim and research questions

The overarching aim of this thesis is to quantify the impact of the 2018 summer heatwave on emissions from natural systems and how these emissions impact atmospheric chemistry. This is defined further in the research questions below:

- How were emissions from vegetation (BVOC) affected by the drought of 2018 summer compared to the reference year (2017)?
- How did the emissions from vegetation and wildfires affect the atmospheric chemistry/concentration of BVOC, NO_x, O_3, OH, NO_3 and SOA during the summer of 2018?
- How well do the models describe the ecosystem response and impact on atmospheric chemistry compared to measurements of atmospheric concentrations?

As one of the aims is to compare models with measured data, the thesis will primarily focus on southern Finland, as the SMEAR II station in Hyytiälä provides the only available open access dataset of BVOC measurements for this period.

2 Background

2.1 2018 Drought and Wildfires

During the summer of 2018, northern Europe was struck by a heatwave as a result of long-lasting high pressure dominated weather. Sweden experienced unusually high monthly average temperatures for May and July compared to the observed climate, while temperatures in June and late August was more moderate (Wilcke et al., 2020). Similarly, Finland experienced high temperature anomalies in May and July relative to the 1981-2010 climatology (Sinclair et al., 2019). In May, the temperature anomalies were relatively spatially uniform, with higher positive sunshine anomalies in the south, while for July, positive temperature and sunshine anomalies were stronger in northern Finland. Still, absolute temperatures were higher in southern Finland in July. Sinclair et al. (2019) attributed these heatwaves as facilitated by the increased incoming solar radiation due to unusually clear skies, in part because the temperature increase was noticeable in the whole atmospheric column rather than only at surface level.

High temperatures combined with low precipitation, resulted in severe drought in many northern European countries (Krikken et al., 2021). This drought resulted in a high number of wildfires in Sweden, where both amount of fires and the total burnt area (BA) (20 000 ha) were significantly higher than in previous years (2008-2017). Finland also experienced numerous wildfires, burning a total area of 12 000 ha (Lehtonen and Venäläinen, 2021). The high temperatures and drought in Sweden also provided an environment for bark beetles, which killed about 1.1% of Swedish forests in the following years (Jaakkola, 2024). Further, unusually high near-surface ozone levels were recorded.

Numerous studies has attributed the 2018 heatwave to climate change. Thorough model simulations, Wilcke et al. (2020) found that the likelihood of temperatures such as those observed in 2018 has increased since the pre-industrial era. However, for 2018 specifically, Krikken et al. (2021), found high uncertainty in climate change attribution, as fire-characteristics are highly dependant on the chosen model. However, there are many studies that support that extreme weather events, such as the drought and fires during the 2018 summer are predicted to increase in intensity and or frequency with increasing temperatures.

In summary, both Sweden and Finland experienced high temperatures and wildfires during the summer of 2018. Anomalies compared to the climatological mean was largest in May and July, while June and August milder. For Sweden, this further lead to bark beetle outbreaks as well as increased levels of near surface ozone.

2.2 Emissions from Vegetation

2.2.1 Biogenic Volatile Organic Compounds and Plant Stress

Biogenic Volatile Organic Compunds (BVOC) are hydrocarbons emitted from the biosphere to the atmosphere. They are usually defined as molecules with low molecular weight, mostly lipophilic with high vapour pressure in ambient temperatures (Šimpraga et al., 2019). BVOC make up about 90% of global VOC emitted, making the biosphere the main source of VOC to the atmosphere. Forests are responsible for the larger part of global BVOC emissions, with estimates showing that tropical forests contribute to about 70% of these emissions (Šimpraga et al., 2019). In contrast, boreal and temperate forests, which are dominating in Europe, are responsible for 10% of global BVOC emissions. However, other estimations suggest that the contribution from the European boreal forests might be underestimated, especially for terpenes and sesquiterpenes.

About 1-2% of the carbon bound through net primary production is reemitted as BVOCs (Šimpraga et al., 2019). For many tree species, the dominating BVOCs are isoprene (C_5H_8) and monoterpenes ($C_{10}H_{16}$). Together they make up the majority of total emitted VOC, making them the globally

most important BVOCs . Isoprene alone makes up about 50% of total emitted BVOC (Guenther et al., 2012), and is thus the globally dominant BVOC, however, in Boreal forests, monoterpenes are the dominating BVOC (Artaxo et al., 2022)

The production of BVOCs is closely linked to photosynthesis, and typically increases with light availability and temperature. Hence, BVOC emissions follows a diurnal cycle with higher emissions during the day, and lower to no emissions during the night. Similarly, BVOC emissions follow a seasonal cycle with the highest emssions during spring and summer. However, some plants have the ability to store certain BVOC in resin ducts or glands (Jaakkola, 2024), to be emitted at a later stage, more favourable for the plant. This is common for monoterpenes but less so for isoprene, hence the sometimes observed light independance of monoterpene emissions (Schurgers et al., 2009), and stronger light dependence of isoprene. While all plant organs have the ability to produce and emit BVOC's, leaves and needles are the most important plant organs when considering BVOC emissions to the atmosphere (Šimpraga et al., 2019).

BVOC emissions play a key role for plant and ecosystem survival, and is a way in which plants interact with their environment. Emitted BVOCs attract pollinators that recognize the composition of a specific species, and are in this way important for plant reproduction (Jaakkola, 2024). When subject to biotic stress such as herbivores or pathogens, plants can alter their BVOC emissions in order to repel, damage or attract natural predators to attacking organisms. Altered BVOC emisisons can further serve as warning signals to surrounding plants, that can respond, or prepare for a faster response upon attack. Similarly, plants alter their BVOC emissions when subject to abiotic stress such as high temperatures or elevated ozone levels (oxidative stress). Changes in BVOC emissions due to biotic or abiotic stress is often referred to as *induced* emissions, while the continuous emissions are referred to as *constitutive* emissions (Grote et al., 2019). Induced emissions often include green leaf volatiles such as alchohols, aldehydes and acetate. Isoprene and monoterpenes may also be induced, but may also be downregulated in favour of green leaf volatiles. Due to limited studies on the subjects, models generally do not represent induced emissions of BVOC well. For example, when studying the effect of the 2018 heatwave on isoprene emissions in a UK woodland, model algorithms tended to underestimate emissions with 20-40% (Otu-Larbi et al., 2020).

2.2.2 Wildfire Emissions

Wildfires have significant impacts on local and regional air quality, as well as the global climate, due to their emissions of trace gases and particles. Wildfire plumes contain, among other pollutants, large amounts of nitrogen oxides (NO_x), carbon monoxide (CO), carbon dioxide (CO_2), methane (CH_4), nitrous oxide (N_2O), and VOCs (Xue et al., 2024). Some of these are important greenhouse gases, such as CO_2 and CH_4, and thus facilitate global warming. Further, NO_x can react with VOCs to form O_3, which is also a greenhouse gas, as well as harmful for humans and vegetation.

Wildfires also emit black carbon particles, which can absorb solar radiation and thus warm the atmosphere, resulting in positive RF. Further, the particles can deposit on white and snowy surfaces and hence lower the earth albedo, also resulting in positive RF. However, these particles and their climate effect are not covered in this study, as this study focuses on quantifying the atmospheric processes and reactions of BVOCs.

2.3 Atmospheric Processes

BVOC are highly reactive and their lifetime typically spans from minutes to days (Boy et al., 2022). In the atmosphere, BVOC are oxidized through complex reactions by atmospheric oxidants such as ozone (O_3), hydroxyl radicals (OH) and nitrate radicals (NO_3), to form Highly Oxygenated organic Molecules (HOM) (Gagan et al., 2023). Some of these compounds may contribute to initial stages

of atmospheric new particle formation (NPF) involving clustering of individual molecules and the majority will condense onto existing aerosol particles and contribute to their growth and the secondary organic aerosol (SOA) mass concentrations, as described in sections below. Once particles are formed, they grow by condensation and are depleted either though coagulation with larger particles (mostly small particles) or deposition.

Atmospheric aerosol particles generally have a cooling effect on the climate. Incoming solar radiation contribute to warming when it reaches the earth surface, but aerosol particles in the atmosphere with a diameter similar to or larger than the wavelength of solar radiation (ca 300nm), scatter solar radiation and hence, less radiation reaches the earth. This is commonly referred to as the direct effect. Further, particles in the atmosphere larger than about 50nm may act as Cloud Condensation Nuclei (CCN) by lowering the relative humidity required for water to condense. Through this effect, the particles can enable cloud formation. Further, they can also increase the cloud droplet number concentration (CDNC) which leads to brighter clouds with higher reflectivity. Yli-Juuti et al. (2021) demonstrated (from observational data) a strong correlation between emissions of BVOC and occurance of CCN, as well as increased cloud reflectivity. This is often referred to as the indirect effect.

Apart from NPF and SOA formation, oxidation of BVOC affects the atmospheric composition as it depletes the atmosphere (locally) of atmospheric oxidants which lowers the oxidizing capacity of the atmosphere and can affect the lifetime of other compounds. OH, for example, plays an important role in the oxidation of the strong greenhouse gas methane (CH_4). Thus, the depletion of OH can prolong the lifetime of this greenhouse gas and thus have a warming effect (Boy et al., 2022). This effect is mostly local and will primarily affect methane oxidation in the boreal region. OH also oxidizes sulphur dioxide (SO_2) to form sulphuric acid (H_2SO_4), which is considered to be the main nucleating species in the atmosphere and thus responsible for the larger part of NPF (Shan-Hu et al., 2019). OH depletion from BVOC oxidation might in this way also lower the amount of new particles formed (Weber et al., 2022).

Similar to OH, ozone is also depleted through oxidation of BVOC. However, oxidation of BVOC in the presence of NOx can lead to net formation of tropospheric ozone (O_3) (Weber et al., 2022). Tropospheric ozone is a strong greenhouse gas, and has a warming effect on the climate. Furthermore, it is harmful for both human and ecosystem health and causes oxidative stress on plants (which, as mentioned, can alter their BVOC production and emission).

It remains uncertain if the negative RF (cooling) from SOA formation and NPF outweighs the positive radiative forcing (warming) from O_3 formation and prolonged lifetimes of CH_4, as there are studies supporting both possible scenarios (Weber et al., 2022).

2.3.1 Atmospheric Particles

Atmospheric particle size distribution almost always consists of several generally approximately lognormal distribution modes (Hinds, 1999), seen in Table 1.

Particle size often determines the processes in which particles partake, and thus, the lognormal modes can be related to different formation and transformation mechanisms, also shown in the table. These processes are further explained in the following sections. Commonly, the smaller size modes (nucleation mode and Aitken mode) dominate in number distribution while larger modes (accumulation mode and coarse mode) dominate volume or mass distributions.

Table 1: Overview of atmospheric particle size distribution modes, their atmospheric formation mechanisms and sinks. Modes are listed from smallest to largest.

Mode	Formation Mechanisms	Sinks
1. Nucleation	NPF	Growth by condensation to Aitken mode, Coagulation with larger size particles
2. Aitken	Growth by condensation from nucleation mode	Growth by condensation to accumulation mode, Cloud activation
3. Accumulation	Growth by condensation from Aitken mode, Cloud activation of Aitken mode	Wet deposition
4. Coarse	Mechanical generation	Sedimentation

2.3.2 New Particle Formation

New particle formation (NPF) is the formation of new nanosized particles from gas-phase compounds (Shan-Hu et al., 2019). It can be described as a two-stage process, in which 1) a critical nucleus is formed, followed by 2) growth by condensation of said nucleus. According to classical nucleation theory, a prerequisite for the formation of the critical nucleus is the supersaturation of the nucleating compounds/substances. They must be supersaturated enough to exceed the so-called nucleation/free energy barrier (where $\Delta G > 0$).

Classical nucleation theory (CNT) describes the nucleation rate, that is, the number of stable critical clusters formed per unit time (N), as per the equation below:

$$J = \frac{dN}{dt} = J_0 exp(\frac{-\Delta G^*}{kT}) \quad (1)$$

where J_0 is the pre-exponential nucleation rate, ΔG^* the minimum free energy required to form stable clusters, T temperature and k Boltzmann's constant.

Even when a critical nucleus is formed, its growth is limited by the Kelvin effect. The Kelvin effect describes how the vapour pressure over a curved surface is elevated compared to a flat surface due to weakened bonds between molecules. This effect is particularly affecting small particles, thus limiting their growth.

The most common nucleating compound is sulphuric acid (H_2SO_4) (together with, for example ammonia (NH_3)) due to its relatively low vapour pressure under typical atmospheric conditions (Shan-Hu et al., 2019). H_2SO_4 is produced from oxidation of sulphur dioxide (SO_2), which is, as mentioned, mainly oxidized by OH in the gas-phase. Some empirical studies suggest that BVOC oxidation products can nucleate with H_2SO_4 and thus contribute to NPF, but this contribution is highly uncertain. It has also been suggested that isoprene might inhibit NPF due to inhibition of OH production, however these mechanisms are unclear.

As shown by Roldin et al. (2019), NPF can somewhat reduce the climate cooling effect of biogenic SOA (direct effect), and hence, contribute to warming. NPF contributes to a large increase in smaller particles, which BVOC oxidation products are able to condense onto. This means that the organic mass will be distributed among more, smaller particles rather than a few large particles. The smaller particles are less efficient both at scattering light (direct effect) and as CCN (indirect effect), as they require a higher supersaturation in order to activate cloud droplets.

2.3.3 Condensation and SOA Formation

Secondary organic aerosol (SOA) is formed when organic oxidation products (commonly BVOC oxidation products) condense onto particles in the atmosphere, contributing to their growth, and thus, increase in mass (Mahilang et al., 2021). SOA refers to the organic mass fraction of these particles. This formation mechanism separates SOA from primary organic aerosols, which are organic particles emitted directly at the source (for example through combustion) (Jimenez et al., 2009). SOA formed from biogenic precursors (such as BVOC) are referred to as biogenic SOA, but as they are the main focus in the present thesis, they are simply referred to as SOA here.

Condensation is the main atmospheric process that affects particle growth in the atmosphere, in which condensable gases condense onto particles, increasing their mass/volume. The reverse process is evaporation, in which aerosol particles shrink due to gases evaporating from the particle surface. Volume growth rate of a particle (V_p) due to condensation can be described as:

$$\frac{dV_p}{dt} = CR * v_i(c_i - c_{eq,i}) \tag{2}$$

where v_i is the molecular volume of compound i, CR is the collision rate and c_i ans $c_{eq,i}$ is the concentration of compound i in gas-phase and saturation concentration at particles surface, respectively. Aerosol particles contains multiple chemical compounds and water, which results in a lower saturation vapour pressure for a specific compound compared to that of an aerosol particle containing a pure compound, as described by Rault's law. This makes the aerosol particles more stable against evaporation.

2.3.4 Other Processes

Apart from NPF and condensation, particles in the atmosphere are subject to processes of coagulation and deposition, which are briefly described here. It is largely based on the description by Boucher (2015).

Coagulation is the process in which two particles collide and adhere to each other to form a larger particle, thereby reducing the number of particles. Coagulation is thus a result of particle motion, and most common between particles with a large relative size difference due to the high/fast Brownian motion of small particles and the large surface/volume of large particles. Therefore, the primary effect of coagulation is the depletion of smaller particles, as the volume/mass of the new particle will be similar to that of the original larger particle.

Wet deposition is the main sink for atmospheric particles in many regions, especially accumulation mode particles in the atmosphere, which, as the name implies, accumulate in the atmosphere due to ineffective deposition by other processes. Wet deposition can occur in two ways: 1) the cloud activation of a particle, which will fall out as rain (in-cloud scavenging) or 2) the particle impinges on a falling rain droplet below the cloud (below-cloud scavenging). Wet deposition thus depends on size and chemistry of the particle, as well as relative humidity and intensity of rain. Dry deposition is the direct deposition of particles onto the earth surface, and is the main deposition mechanism for particles in areas experiencing little precipitation. Small particles are effectively deposited by diffusion while particles large enough to be subject to the gravitational force are deposited by sedimentation.

3 Methodology

First, an overview of the methods is described. The sections that follow provides a more detailed description of the model setups and runs, as well as the measurement data used for comparison.

3.1 Overview

In order to quantify BVOC emissions, data from two different vegetation models were used. One of the BVOC emission datasets was generated with the Dynamic vegetation model (DVM) Lund-Potsdam-Jena General Ecosystem Simulator (LPJ-GUESS) (daily emissions in 0.5^{o}x0.5^{o} grid resolution). The second dataset used was the CAMS-GLOB-BIO_v3.1 (Copernicus Atmosphere Monitoring Service; Sindelarova et al., 2022), which is calculated using the semi-mechanistic model Model of Emissions of Gases and Aerosols from Nature (MEGAN) (hourly emissions averaged over one month, in 0.25^{o}x0.25^{o} grid resolution). These datasets are hereon referred to as LPJ and CAMS.

To model the atmospheric processes for these emissions, the process based atmospheric model Aerosol Dynamics and gas phase CHEMistry model (ADCHEM) was chosen. ADCHEM requires hourly input data, and thus, emissions from LPJ-GUESS were scaled with CAMS emissions in order to obtain a diurnal profile (described in detail in the section below). In order to allow comparison with observational data, ADCHEM was set up for the forest measurement station SMEAR II in Hyytiälä, southern Finland, for 2017 and 2018, 2017 serving as a reference year. The model was run for four months (May - August, MJJA), in order to cover May and July, which were the most extreme in terms of temperature, with isoprene and monoterpene emissions from both vegetation models as input. All other emissions used as input to ADCHEM were obtained from CAMS. This allows for easier evaluation for model performance, as the only difference between the model setups are isoprene and monoterpene emisisons.

A schematic overview of the methodology is shown in Figure 2 below. More detailed descriptions of the models and data collection are provided in the sections below.

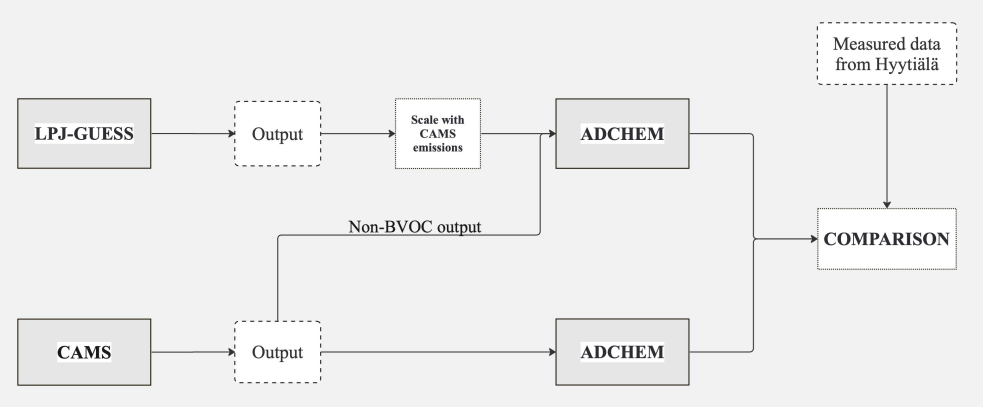

Figure 2: Overview of method

In total, 5 model simulations setups were tested in ADCHEM. As described above, ADCHEM is set up for Hyytiälä measurement station for the years 2017 and 2018, using emissions from both LPJ-GUESS and CAMS. These simulations constitute the first four simulations, and from hereon refered to as CAMS 2017, CAMS 2018, LPJ 2017 and LPJ 2018. These were compared with measurements from Hyytiälä. The model setup that showed the overall closest agreement with observed BVOC concentrations was chosen in order to conduct the last simulations, where BVOC emissions were scaled to better match measured concentrations for the year 2018. Wildfire emissions from GFED4 (Global Fire Emission Database) were included in all model setups.

3.2 Modelling BVOC Emissions

This section describes how BVOC emissions are calculated in LPJ-GUESS and MEGAN. The setup of the LPJ-GUESS model is also described briefly, while the setup of MEGAN used to generate the CAMS dataset is described in detail by (Sindelarova et al., 2022). The models differ in the way that LPJ-GUESS, as a DVM, simulates a multitude of processes in the forest ecosystem, while MEGAN is an emission model and thus needs information about the vegetation from other models or observations.

In order to use modelled LPJ-GUESS concentrations, which are given in mg $m^{-2}d^{-1}$, in ADCHEM, which requires hourly input, these emissions were scaled with the CAMS emissions in order to obtain a diurnal profile. The equation used is shown below.

$$emission_{LPJ}(t) = emission_{LPJ} \cdot \frac{emission_{CAMS}(t)}{mean(\sum_{t=1}^{24} emissions_{CAMS}(t))} \tag{3}$$

3.2.1 LPJ-GUESS

In the present study, the latest version of LPJ-GUESS (LPJ-GUESS v4.1) is used. The framework consists of several modules describing ecosystem state (such as net primary production, structure or composition) and ecosystem processes that affect these states. Fast processes, such as photosyntesis, are simulated daily, while slower processes, such as fire disturbance, are simulated annually. Vegetation in the model is represented by Plant Functional Types (PFTs). For the simulation in this study, the climate dataset ERA-INTERIM was used as input to the model for the period 1900-2018.

The model was first described by Smith et al. (2001). The BVOC production and emission has been described by Schurgers et al. (2009). Hence, only a short overview of how BVOC emissions are simulated is given here.

BVOC production is closely linked to photosynthesis. To calculate production, a fraction of the photosynthetic electron transport, ε, is attributed to terpenoid (BVOC) production. This fraction is calculated as a function of temperature (T), seasonality (σ, in the case of isoprenes) and atmospheric CO_2 concentration, as well as a standard species specific fraction (ε_s), according to the equation below.

$$\varepsilon = f(T)f(\sigma)f([CO_2])\varepsilon_s \tag{4}$$

Then, terpenoid production (I) is calculated as a function of ε, electron flux generated for photosynthesis (J) and the yield of terpenoids for each unit of electron flux (α). Isoprene seasonality is only applied for deciduous PFTs, as evergreen PFTs are assumed not to exhibit any seasonality in their terpene production.

$$I = \varepsilon J \alpha \tag{5}$$

The model accounts for the ability for certain plants to store monoterpenes. This is true for the dominating PFT in boreal forests (coniferous PFT). The storage is handled as a single storage pool. The rate of monoterpene emission ($M_{emission}$) from this storage is temperature dependent, according to the equation below:

$$M_{emission} = \frac{m}{\tau} \tag{6}$$

where m is the size of the storage pool and τ is the temperature dependent time constant.

3.2.2 MEGAN

MEGAN is a semi-mechanistic model used to estimate fluxes of biogenic compounds between terrestial ecosystems and the atmosphere. As the model is described in detail by Guenther et al. (2012), only a brief overview is presented here.

MEGAN uses inputs such as leaf area index, weather characteristics (temperature, solar radiation, water availability) and PFT/species composition to describe the amount of vegetation, factors affecting emissions from vegetation and what kind of vegetation exists. PFT input is based on satelite data. The output, time resolved gridded BVOC emission estimates, is calculated for 19 compound classes. These compound classes include for example isoprene, limonene, 3-carene, α-pinene and *beta*-pinene as separate classes, while some classes include several compounds (with the same emission activity parameterizations). The emission of compound class i, (F_i, in $\mu g m^{-2} h^{-1}$), is calculated as described in Equation 7 below,

$$F_i = \gamma_i \sum \eta_{i,j} \chi_j \tag{7}$$

where γ_i is the emission activity factor, accounting for the processes controlling emission response for the specific compound class, $\eta_{i,j}$ is the compound class emission factor for standard conditions for vegetation type j, and χ_j is the fractional grid box areal coverage of vegetation type j. The activity factor accounts for emission response to leaf area index (LAI), light ($\gamma_{\mathrm{P,i}}$), temperature ($\gamma_{\mathrm{T,i}}$), leaf age ($\gamma_{\mathrm{A,i}}$), soil moisture ($\gamma_{\mathrm{SM,i}}$) and CO_2 inhibition ($\gamma_{\mathrm{C,i}}$), as seen in the equation below:

$$\gamma_i = C_{CE} \cdot LAI \cdot \gamma_{P,i} \cdot \gamma_{T,i} \cdot \gamma_{A,i} \cdot \gamma_{SM,i} \cdot \gamma_{C,i} \tag{8}$$

where C_{CE} is the canopy environment coefficient is an assigned value resulting in $\gamma_{\mathrm{i}} = 1$ for standard conditions.

3.3 Modelling Atmospheric Processes with ADCHEM

ADCHEM is a Lagrangian chemistry transport model (Roldin et al., 2011). In the present work, ADCHEM was run as a 1D-column model along pre-calculated air mass trajectories from the HYSPLIT model arriving at Hyytiälä every 18th hour. The vertical column, which extended from the surface to 2.5 km above the ground level, was represented by 20 grid cells, illustrated in Figure 3 below.

ADCHEM models the dynamics of the gas-cluster-aerosol system by combining an aerosol module which treats atmospheric aerosol processes such as condensation, evaporation, coagulation, dry deposition and in- and below cloud processing and scavenging with a molecular cluster dynamics module (ClusterIn, Olenius and Roldin, 2022). In the present work, NPF is modelled through the formation of the following molecular clusters:

- $H_2SO_4 - NH_3$ (ammonia)
- $H_2SO_4 -$ DMA (dimethylamine)
- $HIO_2 - HIO_3$ (iodous acid)
- $HIO_3 -$ DMA

This has been described in detail by Olenius and Roldin (2022) and Xavier et al. (2024).

Further, ADCHEM includes detailed gas-phase chemical oxidation mechanisms for the BVOCs isoprene, α-pinene, β-pinene, Δ3-carene and D-limonene, and oxidation of these by OH, O_3 and NO_3. The SOA formation is represented by the condensation of about 900 condensable organic vapors included in the gas-phase chemistry mechanism.

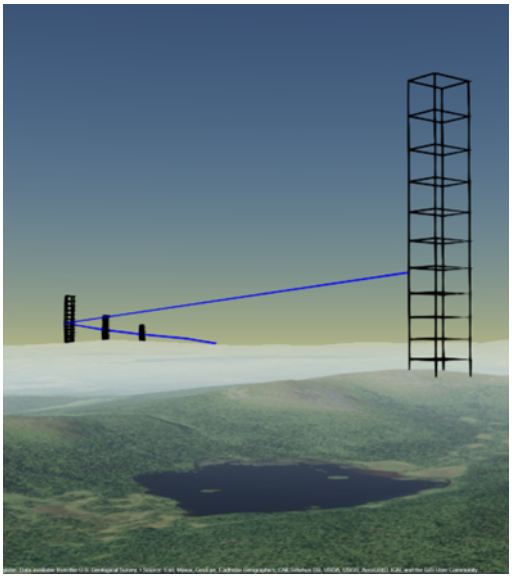

Figure 3: Illustration of the ADCHEM 1D column along an air mass trajectory by Robin Wollesen de Jonge

Inputs in the model, along the HYSPLIT air mass trajectories, are:

- meteorological data (rainfall intensity, vertical temperature and RH profiles, mixing height and wind speed at two altitudes within the surface layer) from NOAA Global Data Assimilation System (GDAS).
- emissions of BVOC from either CAMS or LPJ-GUESS
- emissions of anthropogenic non-methane VOCs (NMVOCs), NOx, SO2, carbon monoxide (CO), ammonia (NH3), and size resolved primary particle emission factors from CAMS, derived based on CAMS PM2.5 emission factors.

3.4 Observational Data

All observational data (NOx, Ozone and BVOC concentrations, and Particle Number Size Distribution) were obtained from the SMEAR II station in Hyytiälä, southern Finland (61°51 N, 24°17 E, see Figure 4). The station is part of the SMEAR (Stations for Measuring the forest Ecosystem-Atmosphere Relationships) network, and has been operating since 1995 (Junninen et al., 2009). The station is located in a forest stand established in 1962, dominated by Scots pine (*Pinus sylvestris*), with mixture of Norway spruce (*Picea abies*) and scattered deciduous trees, (Hari and Kulmala, 2005), representing a boreal coniferous forest. The stand is surrounded by managed coniferous forest stands of different ages.

The station was chosen as it has long-term measurements of BVOC concentration for the years studied (2017-2018). Observational data was collected from EBAS (ebas.nilu.no; particle number size distribution; Kumala and Petäjä, 2024) and smartsmear (smear.aava.csc.fi; ozone, NOx and BVOC concentrations; Aalto et al., 2023).

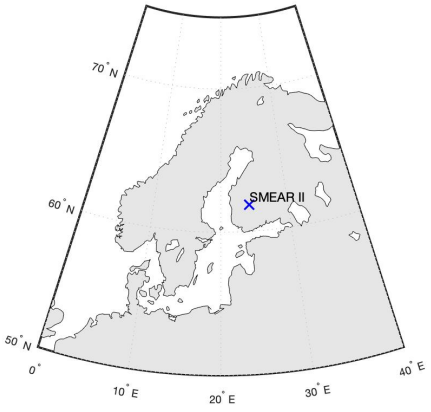

Figure 4: Map of northern Europe, the blue cross marks the location of SMEAR II Hyytiälä in southern Finland

3.4.1 Measurement Instruments

At SMEAR II, NO_x, O_3 and BVOC concentrations are measured at a 128 m high tower, reaching both into and above canopy. NO_x and O_3 are measured with a chemiluminescence analyzer and an ultraviolet light absorption analyzer, respectively. Isoprene and monoterpene concentration are measured with the PTR-MS technique. Measurements, calibration and volume mixing ratio calculations has been described in detail by Kulmala et al. (2008) and will not be described in detail here. The PTR-MS only detects masses of compounds, meaning that BVOC with the same mass (for example isoprene and MBO) cannot be distinguished.

The DMPS measures the total concentration particle number size distribution (Kulmala et al., 2011). The setup at SMEAR II consists of two DMPSs with partly overlapping size ranges, each consisting of a bipolar charger, a Differential Mobility Analyzer (DMA) and a Condensation Particle Counter (CPC). The setup is able to detect particles from 3 - 1000 nm. The bipolar charger provides the aerosol sample with a known charge distribution. In the DMA, a fraction of the particles in the aerosol sample is selected based on their electrical mobility. The selected particles are grown by condensation to detectable sizes and counted in the CPC. By repeating this process and changing the voltage of the DMA, the sample can be sorted according to the electrical mobility of the particles, and a number size distribution can be obtained. Table 2 presents the measured compounds, as well as the instruments used to measure them.

Table 2: The table shows an overview of the measured data used for comparison with the models, and the instrument used to measure the data.

Measured variable	Instrument	Unit
Particle Number Size Distribution (dN/dlogDp)	DMPS (differential mobility particle sizer)	cm^{-3}
Ozone concentration (O_3)	TEI 49 C ultraviolet light absorption analyzer	ppb
Isoprene + MBO (C_5H_8)	Proton-transfer-reaction mass spectrometry (PTR-MS)	ppb
Monoterpenes ($C_{10}H_{16}$)	Proton-transfer-reaction mass spectrometry (PTR-MS)	ppb
Nitrogen oxide concentration (NO_x)	Ecophysics CLD 780 TR chemiluminesence analyzer	ppb

4 Results

4.1 Emissions from Vegetation and Forest Fires

Monthly mean isoprene and monoterpene emissions from LPJ-GUESS for 2017 and 2018 were compared with a reference period, consisting of monthly mean emissions over the years 2003-2016. Figures 5 show isoprene and monoterpene emissions in July for both years, divided by the monthly mean from the reference period. The figures clearly illustrate a strong increase in both monoterpene and isoprene emissions in 2018, compared to a decrease in emissions in 2017 (for northern Europe, specifically Finland). The same trend is seen for all months (see Figure 19 - 22 in Appendix A), with the largest difference in emissions in May and July 2018.

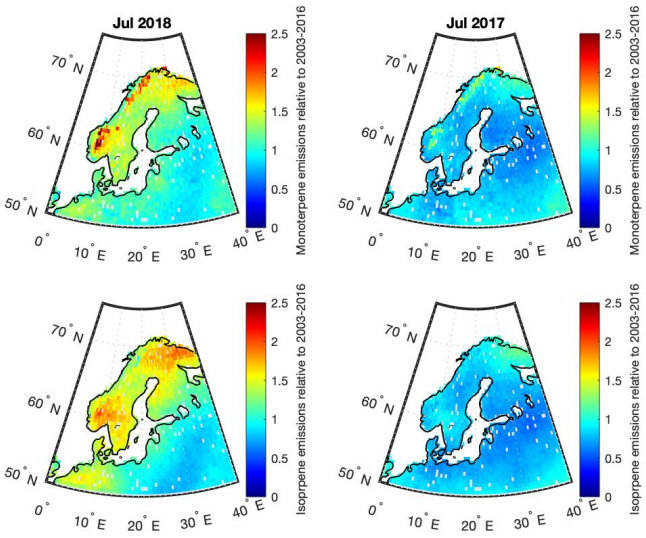

Figure 5: Average isoprene and monoterpene emissions for July 2017 and 2018, divided by average respective emisisons for July 2003-2016.

Figure 6 shows cumulative emissions of isoprene, total monoterpenes and α-pinene along the HYSPLIT trajectories in July 2017 and 2018 (start 3 h before reaching the SMEAR II station) from CAMS compared to the emissions from LPJ-GUESS. While total monoterpene and α-pinene emissions are slightly higher in CAMS, isoprene emissions are substantially higher in LPJ-GUESS. The same trend can be seen for May, June and August (see Figure 23 - 25 in Appendix A). Both models show an increase in BVOC emissions in 2018 compared to 2017. Cumulative emissions along the whole trajectories (11 days before reaching the SMEAR II station, covering northern Europe) showed increased emissions in June-August in 2018, while emissions in May were similar. These also show that isoprene emissions are much higher in LPJ-GUESS, and that total monoterpene emissions are somewhat higher in CAMS.

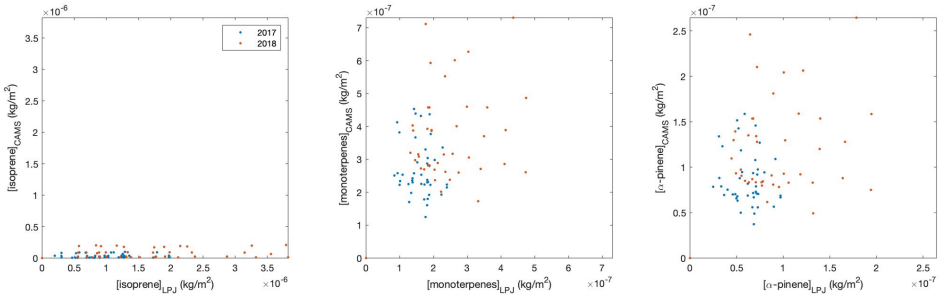

Figure 6: Cumulative emissions from LPJ-GUESS along HYSPLIT airmass trajectories plotted against cumulative emissions from CAMS, starting 3 h from the Hyytiälä measurement station (July 2018 and 2017)

4.2 Atmospheric Composition and Chemistry

This section presents the results from the ADCHEM model runs. This includes the concentration of BVOC, O_3, NO_x, OH and NO_3 as well as the particle number size distributions. Results are presented as to provide easy comparison between both the different years, but also between the different BVOC emission products (LPJ and CAMS) and with observational data. Figures with the modelled timeseries for all compounds can be found in Appendix B.

Figure 7 compares the median isoprene and monoterpene concentration at the lowest measured and modelled layers (4.2 m and 5 m respectively) for all months (MJJA). Both measured and modelled concentrations show higher concentrations during 2018, with the exception of monoterpenes in June, which is higher in 2017. Both measured and modelled emissions show the most significant difference in BVOC emissions in July. The models generate a stronger increase in May concentrations between 2017 and 2018 compared to the measured concentrations, particularly for isoprene. The isoprene concentration modelled with LPJ-GUESS emissions is significantly higher than both the concentration modelled with CAMS emissions and the measured concentration. The difference between modelled and measured isoprene and monoterpene concentrations is illustrated further in Figure 8 below. The factor of deviation from measured concentrations of isoprene and monoterpenes, for all months and model setups, are shown in Tables 3 and 4 in Appendix B.

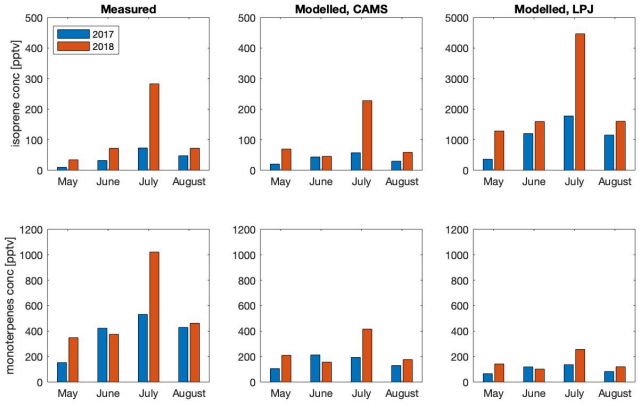

Figure 7: Measured and modelled BVOC concentrations at the lowest measured and modelled layers (4.2 and 5 m respectively) for 2017 and 2018. Note that the y-axis for isoprene modelled with LPJ-GUESS emissions has a y-axis 10 times greater than measured isoprene and isoprene modelled with CAMS emissions

The largest deviation from measured BVOC concentrations is the isoprene concentration using emissions from LPJ-GUESS, which overestimates isoprene with a factor between 15.8 and 37.6. The largest deviation in modelled concentration relative to measured concentration is observed in May 2018 (Table 4, Appendix B), while the largest difference in value is observed in July 2018 (Figure 8b). CAMS instead underestimates the isoprene concentration for all months except May. Both model setups underestimate monoterpene concentration in the forest canopy, LPJ-GUESS more so than CAMS. In 2018, the highest modelled concentration of monoterpenes is in July, followed by May, while measured concentrations, while highest in July, is lowest in May. In 2017, modelled concentrations with CAMS emissions show highest monoterpene concentrations in June, while both measured and modelled concentrations with LPJ-GUESS emissions both show the highest concentrations in July.

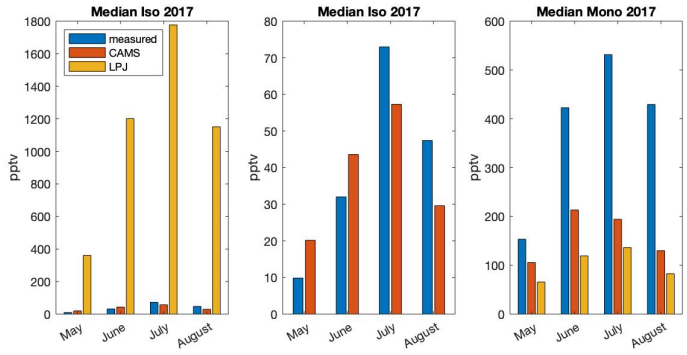

(a) 2017

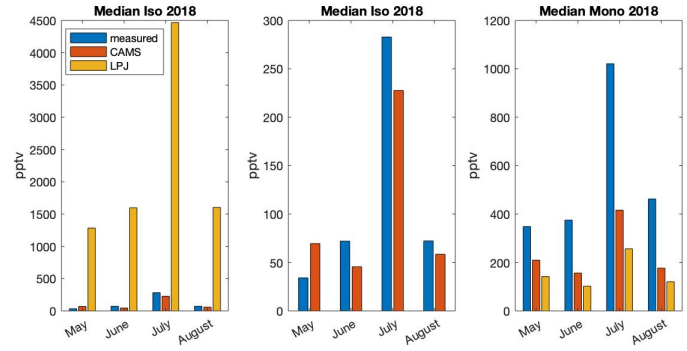

(b) 2018

Figure 8: Modelled and measured median isoprene and monoterpene concentrations at the lowest measured and modelled layers (4.2 and 5 m respectively) at Hyytiälä during summer months (MJJA) for (a) 2017 and (b) 2018.

The measured and modelled particle number size distributions, shown in Figure 9 (CAMS setup) and Figure 10 (LPJ-GUESS setup), show that the models underestimate the number of particles present at the station. This underestimation is more severe for 2018. The measured particle number size distribution contains a higher number of particles in 2018 for all months, however, in May and July, the particle volume increases with a factor of 1.9 and 2.9 respectively (see Table 5 in Appendix B). This increase in volume is somewhat captured in both model setups for May, but not in July. Notably, the modelled emissions show more particles in nucleation mode (< 10 nm) in 2017. In 2018, only the model setup with LPJ-GUESS emissions show these small particles. Figure 26 and 27 in Appendix B show that the difference between the two different model setups is small for both years.

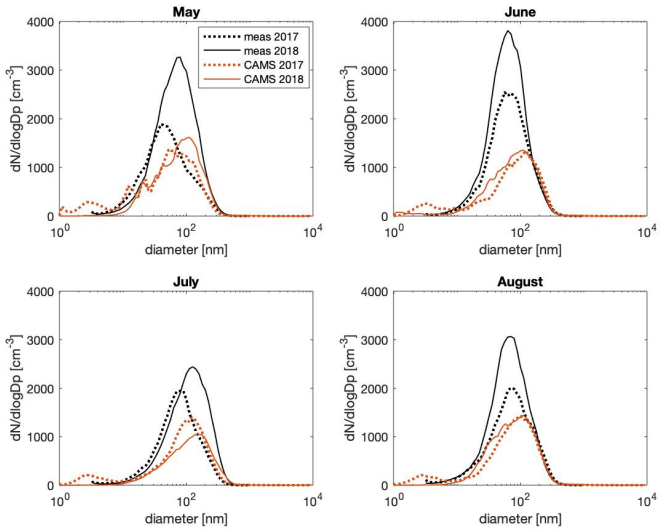

Figure 9: Comparison between modelled (CAMS setups) and measured median particle number size distribution at Hyytiälä, summer months, 2017 and 2018 (MJJA).

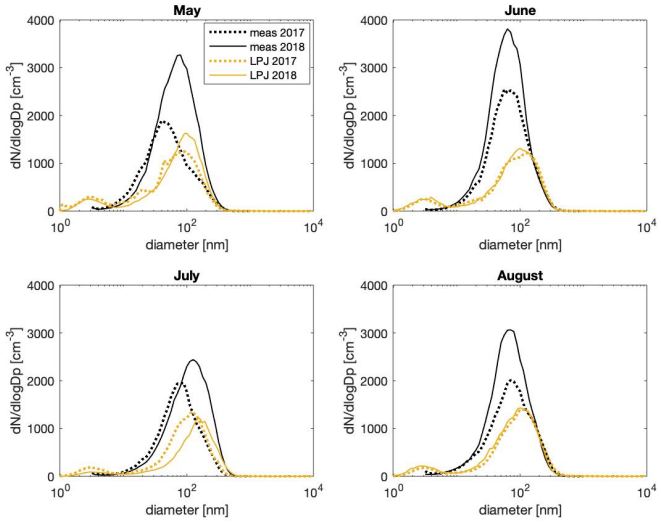

Figure 10: Comparison between modelled (LPJ setups) and measured median particle number size distribution at Hyytiälä, summer months 2017 and 2018 (MJJA).

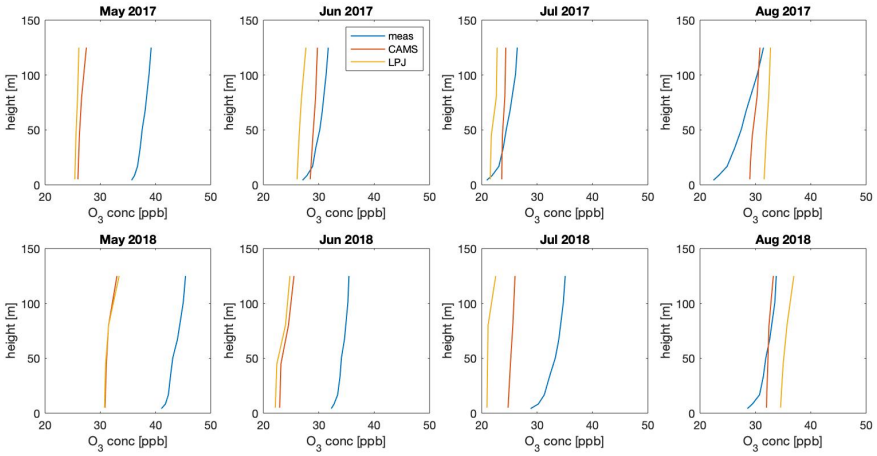

Figure 11: Comparison between modelled (LPJ and CAMS setups) and measured ozone concentrations up to 125 m height for summer months (MJJA) 2017 and 2018.

Figure 11 shows the modelled and measured ozone concentrations at Hyytiala for summer months, year 2017 and 2018. Overall, the models lack the slight decrease in ozone close to the ground. The measured ozone concentration is higher in 2018 than in 2017, and is highest in May for both years. This trend is not well represented by either model setup. Comparing the two model setups, the LPJ setup generates a similar or lower O_3 concentration in May - July, and a higher concentration in August, compared to the CAMS setup. Both years show this trend. In 2018, both models show the highest O_3 concentration in May and August.

The modelled NO_x concentration is lower in setups using LPJ-GUESS emissisons compared to setups using CAMS emissions (see Figure 12). While the measured concentration is similar or higher in 2018 compared to 2017, models show similar or lower concentrations of NO_x. In 2017, both models tend to overestimate the concentration of NO_x, while models underestimate NO_x in May and June 2018.

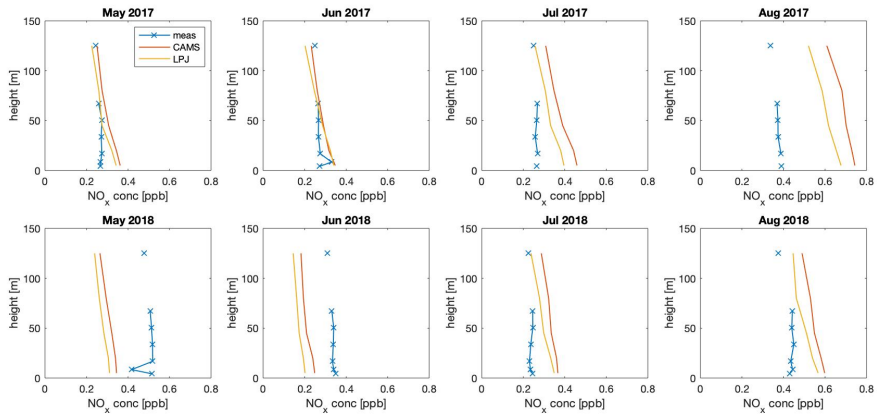

Figure 12: Comparison between modelled (LPJ and CAMS setups) and measured NO_x concentrations up to 125 m height for summer months (MJJA) 2017 and 2018. Note the difference in x-axis between the years

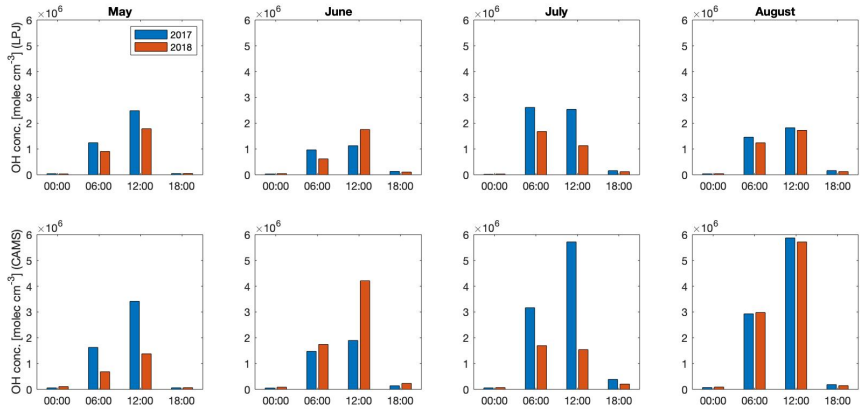

Figure 13: Diurnal variation of the median OH concentration, modelled with LPJ-GUESS emissions (above) and CAMS emissions (below) at SMEAR II. Time (x-axis) is given in UTC. Note the difference between y-axis scale for the OH concentration modelled with CAMS.

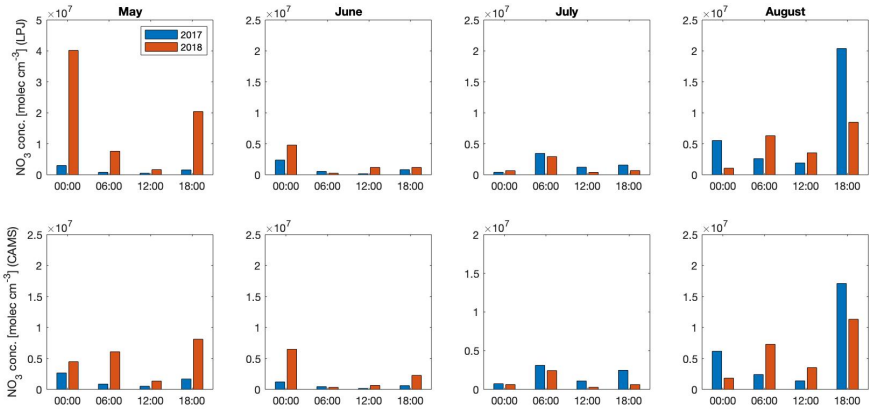

Figure 14: Diurnal variation of the median NO_3 concentration, modelled with LPJ-GUESS emissions (above) and CAMS emissions (below) at SMEAR II. Time (x-axis) is given in UTC. Note the difference in the y-axis for May modelled with LPJ-GUESS emissions.

Figures 13 and 14 shows the difference in the modelled OH- and NO_3 concentrations between the years, respectively. Both model setups yield higher concentrations of OH during the day, for both years. In May and July 2018, the concentration of OH decreases compared to 2017. This decrease is largest for the CAMS setup, while the LPJ-GUESS setup produces overall lower concentrations than the CAMS setup.

There is no clear trend, either increase or decrease in the concentration of NO_3 between the years. Notably, NO_3 increases significantly in May 2018 in both model setups compared to May 2017. For all months in 2017 except July, the concentrations show a diurnal cycle with higher concentrations during nighttime. This can be seen for some months in 2018 for example June, CAMS emission setup, and May, LPJ-GUESS emission setup. However, in August 2018, both setups, and July, both years and setups, the NO_3 concentration is high at 06:00 (UTC, 08:00 local time). In July, there is a decrease in NO_3 concentration between the years, for both models.

4.2.1 CAMSx2: Increased Monoterpene Emissions in CAMS

In order to investigate if higher emissions of BVOC would result in a better representation of atmospheric chemistry, monoterpene emissions from CAMS 2018 were multiplied with a factor of two in ADCHEM. This model setup is hereon referred to as CAMSx2. Only monoterpene emissions were scaled, as isoprene concentrations were sufficiently captured by the model. Figures with the modelled timeseries for all compounds can be found in Appendix C.

When running ADCHEM for 2018 with CAMSx2 monoterpene emissions, both isoprene and monoterpene emissions increase (see Figure 15). This model setup results in higher than measured monoterpene concentrations, with the largest difference in May and July. The same can be seen for isoprene concentrations, with the exception of June. Even though monoterpene emissions were scaled with a factor of two, the resulting modelled concentrations are almost three times higher when using increased emissions (for July).

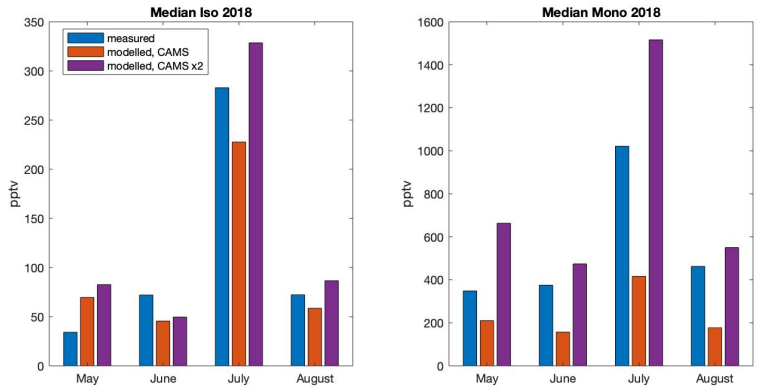

Figure 15: Comparison between measured and modelled (CAMS and CAMSx2) BVOC concentrations at Hyytiälä for summer months (MJJA) 2018.

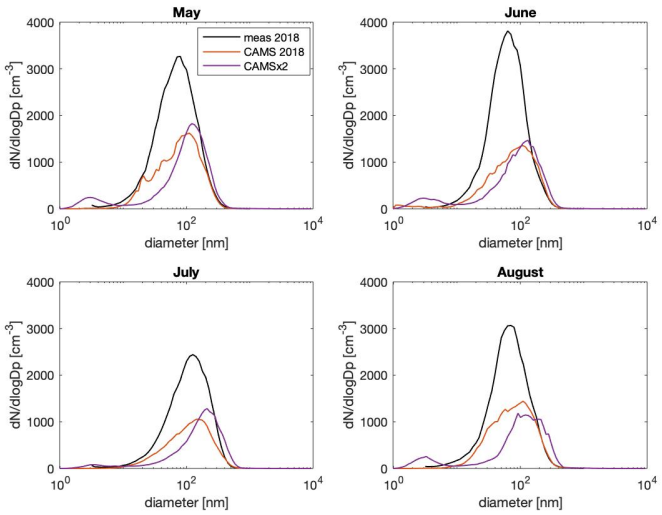

Figure 16: Comparison between modelled (CAMS and CAMSx2) and measured median particle number size distribution at Hyytiälä, 2018 (summer months, MJJA)

The particle number size distribution modelled with doubled CAMSx2 emissions is not substantially different than that modelled with CAMS emissions. Compared to the CAMS model setup for 2018, the particle volume increases for all months, particularly in July where it increases with a factor of 2.03 (see Figure 16 and Table 6 in Appendix C). Further, more particles in nucleation mode are present.

Increased CAMS BVOC emissions in ADCHEM produce a lower concentration of both NO_x and O_3 (see Figure 17). In 2017 as well as in May and June 2018, both model setups yield a lower concentration of O_3 compared to the measured concentration, while producing a higher than modelled concentration in July and August 2018. Figure 18 show the modelled median concentration of atmospheric oxidants OH and NO_3 modelled using CAMS 2018, LPJ-GUESS 2018 and CAMSx2 BVOC emissions. For both the CAMS and CAMSx2 setups, the OH concentration is lowest in May and July, while the LPJ-GUESS setup produces similar concentrations for all months. In June and August, CAMS produces the highest OH concentration, while LPJ-GUESS produces the lowest. For May and July, the CAMSx2 setup produces the lowest concentration. The CAMSx2 setup produces the lowest concentration of NO_3 for all months (although is similar to concentrations from the LPJ-GUESS setup in August). It exhibits similar diurnal trends as the CAMS 2018 setup.

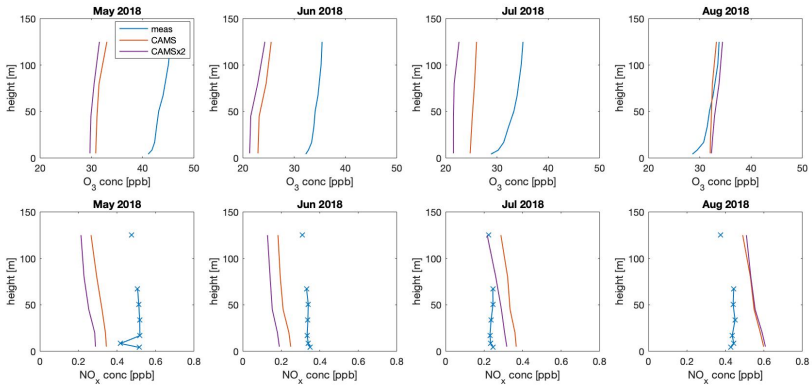

Figure 17: Comparison between measured and modelled (CAMS and CAMSx2) O_3 and NO_x concentration, up to 125 m height for summer months (MJJA) 2017 and 2018.

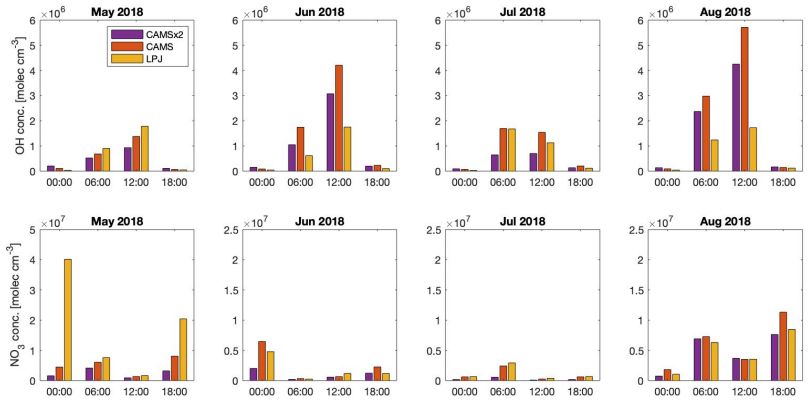

Figure 18: Diurnal variation of the median OH and NO_3 concentration for all model setups (CAMS, CAMSx2 and LPJ), 2018 at SMEAR II. Time (x-axis) is given in UTC. Note the difference in the y-axis for May modelled with LPJ-GUESS emissions.

5 Discussion

5.1 Response of BVOC Emissions to the 2018 Drought

BVOC emission data from LPJ-GUESS show a strong increase in both isoprene and total monoterpene emissions in Northern Europe in 2018 compared to the reference period (2003-2016), particularly in May and July, which was expected as these months were characterized by unusually high temperature and clear skies, both of which provides good conditions for BVOC production. In 2017, BVOC emissions are slightly lower than the reference period. This is important to keep in mind when analyzing the results, as 2017 is used as a reference year in the present study. The reference period includes years of other severe heatwaves, the central European heatwave of 2003 and the Russian heatwave of 2010, the latter also affecting Finland (Sinclair et al., 2019), which would affect the comparison with the reference period.

Cumulative emissions along the HYSPLIT trajectories show that total monoterpene and α-pinene emisisons are similar in the two BVOC emission datasets used in this study (slightly higher in CAMS for May and June). Isoprene emissions are, however, substantially higher in LPJ-GUESS for both years. As shown in Figure 8, this leads to a severe overestimation of the isoprene concentration at Hyytiälä. Measured data show that monoterpene is the dominating BVOC in Hyytiälä, which is expected of a boreal forest. However, in the model setup using LPJ-GUESS emissions, isoprene is by far the dominating BVOC which is more similar to the BVOC composition in other parts of the world. In contrast, the model setups using CAMS emissions are able to more accurately represent the observed isoprene concentration.

Both model setups capture the observed increase in both isoprene and total monoterpene concentration at Hyytiälä in May and July 2018, while the concentrations in June and August are more similar to the modelled concentrations in 2017. However, both setups underestimate the total monoterpene concentration, LPJ-GUESS slightly more so than CAMS. This could indicate that the vegetation experience stresses not accounted for in the models, for example from bark beetle infestations. In Sweden, the high temperatures in 2018 were accompanied with a bark beetle outbreak, which has been empirically shown to increase BVOC emissions significantly (Jaakkola, 2024).

5.2 Atmospheric Composition

The observed particle size distribution at Hyytiälä contains a higher number of particles in 2018 compared to 2017. Additionally, the particle volume is higher in May and July 2018 compared to 2017, which could indicate that the increase in BVOC emissions lead to formation of SOA. The model setups, however, underestimate the number of particles in the atmosphere, especially for 2018. Furthermore, there are few significant differences in the particle size distribution between the years, except for an increase in particle volume in May (for model setups using LPJ-GUESS and CAMS emissions). In July, the models show a slight decrease of particles. There are few significant differences in the particle number size distributions between model setups, which would indicate that the high concentration of isoprene in the model setup using LPJ-GUESS emissions does not contribute significantly to particle growth. When monoterpene emissions are increased in ADCHEM (CAMSx2), the particle volume increases, especially for May and July (as well as slightly in August), but the total number is still lower than observed particle number concentration. This could indicate that the model has too low emissions of primary particles, or that the representation of NPF is insufficient to capture observed particle number concentrations. This could, for example, mean underestimation of the impact of NPF from organic compounds. Another potential explanation is that particle growth due to increased BVOC emissions increases the condensation sink for compounds such as H_2SO_4, which would otherwise have formed new particles and grown into Aitken mode.

The modelled concentration of atmospheric oxidants OH and NO_3 are lower in 2018 compared to 2017 in May and July (OH) and July (NO_3). The OH concentration exhibits a diurnal trend with higher concentrations during daytime, which is expected as OH is formed though photolysis of O_3.

The decrease in OH concentration between the years indicates that OH is depleted to a higher degree due to increased BVOC emissions. The setup using LPJ-GUESS emissions generates overall lower concentrations of OH. This could be explained by the fact that the LPJ setup has higher total BVOC emissions due to the overestimation of isoprene, which results in higher isoprene concentrations and therefore, OH depletion. Depletion of OH can also explain why both monoterpene and isoprene concentrations increase in the CAMSx2 setup, even when only monoterpene emissions are increased. Higher emissions of monoterpenes lead to a higher total BVOC concentration, meaning that OH is depleted which might lower the oxidation rate of isoprene and monoterpenes. Interestingly, the CAMSx2 setup produces lower concentrations of OH in May and July compared to LPJ-GUESS, while the opposite is true for June and August. This might imply that monoterpenes are oxidized at a higher rate than isoprene, as the variation in monoterpene concentrations over the months seem to have a greater impact on the OH concentration. OH is formed from products from O_3 photolysis, and hence, a lower ozone concentration is expected to yield a lower amount of OH. The O_3 concentration is lower for the CAMSx2 setup compared to the CAMSx2 setup. Hence, the decrease in OH could also be explained by the lowered O_3 concentrations. However, as the only difference between these setups is the increased monoterpene emissions in CAMSx2, this implies that the O_3 concentration might also be depleted by oxidation of BVOC. For further studies on the 2018 summer heatwave, it could be interesting to look at the methane concentration at Hyytiälä, which would be higher if OH is depleted(Boy et al., 2022).

The diurnal variation of NO_3 exhibits, for some months, an increase during nighttime and a decrease during daytime. This can be explained by the fact that during the day, NO_3 is rapidly photolyzed. However this diurnal cycle is not always produced by the model setups, for example in July and August 2018. Notably, the concentration of NO_3 is high in May, especially in the LPJ-GUESS setup. NO_3 is formed through reactions between NO_x and O_3, but neither compound is substantially higher in the LPJ-GUESS setup compared to the CAMS setup. However, the O_3 concentration in LPJ-GUESS is slightly higher in May 2018 compared to May 2017. In the CAMSx2 setup, the NO_3 concentration is slightly lower compared to the CAMS setup for 2018, which might be expected as both NO_x and O_3 concentrations are lower in the CAMSx2 setup.

The observed concentration of O_3 is generally higher in 2018 compared to 2017. This is concurrent with the documented increase in tropospheric O_3 during the 2018 summer in Sweden (Jaakkola, 2024). Observed NO_x concentrations are generally similar between the years, with the exception of May which exhibits a higher concentration in 2018. The models do not capture the increase in O_3 between years, except for in May and partly August, nor the increase in NO_x seen in May 2018. This implies that the actual OH and NO_3 concentration at Hyytiälä might be misrepresented by the models. As models underestimate O_3, particularly in May, June and July 2018, this could imply that OH and NO_3 also are underestimated in the model, which could partly explain the overestimation of the monoterpene concentration in the CAMSx2 setup. It could, however, also be the case that the ADCHEM model underestimates the net formation of O_3 that can occur in high NO_x environments (for example in May 2018).

6 Conclusion and Outlook

As extreme weather events such as heatwaves and drought are expected to increase due to global warming, it is important that models used to predict future climates can sufficiently represent the impacts of such events. The aim of this thesis was therefore to quantify the ecosystem response to the 2018 summer heatwave, and the impact on atmospheric composition. To do this, data from different BVOC emission models were used as input into the atmospheric model ADCHEM. The modelled concentrations of BVOC, O_3 and NO_x were then compared with measurements from the SMEAR II station in southern Finland.

The stress response from boreal forests during the heatwave and drought 2018 caused BVOC emissions to increase during this period. Both BVOC emission datasets used in this study showed increased BVOC emissions during the summer of 2018. These increased emissions lead to higher concentrations of isoprene and monoterpenes, which were particularly high in May and July, which is also concurrent with observed concentrations. However, the model setups tended to underestimate the BVOC concentration, except for the setup using LPJ-GUESS emissions, which greatly overestimated isoprene concentrations. This was caused by very high isoprene emissions in the LPJ-GUESS dataset. The underestimation of monoterpenes in both model setups, for both years, setups implies that monoterpene emissions from boreal forests might be underestimated in MEGAN and LPJ-GUESS, not only during extreme weather events.

The increased emissions of BVOC lead to particle growth, which could be observed in both measured and modelled particle number size distributions. However, the model setups underestimated the amount of particles present in the atmosphere, which indicates either underestimated primary particle emissions, or NPF events in the ADCHEM model. While the observed concentration of O_3 was higher in 2018 compared to 2017 for all months, the observed NO_x increased particularly in May 2018. In May, this could be the result of net formation of O_3 from BVOC oxidation in high-NOx environments, but it is unlikely the case for the other months. The modelled concentrations of these compounds did not generally match the trends. Particularly, O_3 in 2018 is underestimated by all model setups. The modelled concentrations of atmospheric oxidants NO_3 and OH decreased in 2018 for May (only OH) and July (OH and NO_3), which is likely due to depletion though oxidation of BVOC. Both OH and NO_3 formation depend on the concentration of NO_x and O_3, thus, the modelled concentrations of NO_3 and OH may not be representative for the actual concentrations.

Further studies on the subject should investigate the effect of the drought on other boreal forests in Northern Europe in order to draw more general conclusions about the effect of the drought and how well it is represented in models. Studies over longer time periods, especially after 2018 could investigate the prolonged effects of drought, which are expected to decrease BVOC emissions. The ACTRIS station at Hyltemossa has BVOC measurements from 2019, and studies on this site could prove valuable to understand the effects of heatwaves. It would also be good to "crossreference" model setups, i.e running ADCHEM set up for 2017 with emissions from 2018 and vice versa, in order to investigate the influence of meteorology. This could provide further knowledge on both the effect of drought, but also how well models can represent the impact of extreme weather events on ecosystems and atmospheric composition.

References

Aalto, J., Aalto, P., Keronen, P., Kolari, P., Rantala, P., Taipale, R., Kajos, M., Patokoski, J., Rinne, J., Ruuskanen, T., et al. (2023). Smear ii hyytiälä forest meteorology, greenhouse gases, air quality and soil [University of Helsinki, Institute for Atmospheric and Earth System Research]. https://doi.org/10.23729/23dd00b2-b9d7-467a-9cee-b4a122486039

Artaxo, P., Hansson, H.-C., Andreae, M. O., Bäck, J., Alves, E. G., Barbosa, H. M. J., Bender, F., Bourtsoukidis, E., Carbone, S., Chi, J., Decesari, S., Després, V. R., Ditas, F., Ezhova, E., Fuzzi, S., Hasselquist, N. J., Heintzenberg, J., Holanda, B. A., Guenther, A., ... Rizzo, L. (2022). Tropical and boreal forest – atmosphere interactions: A review. *Tellus. Series B, Chemical and physical meteorology*, *74*(1), 24–163. https://doi.org/10.16993/tellusb.34

Berg Malmborg, V. (2014). Anthropogenic influence on new particle formation in the marine boundary layer atmosphere [Student Paper].

Boucher, O. (2015). Atmospheric aerosols, properties and climate impacts. Springer. https://doi.org/10.1007/978-94-017-9649-1_4

Boy, M., Zhou, P., Kurtén, T., Chen, D., Xavier, C., Clusius, P., Roldin, P., Baykara, M., Pichelstorfer, L., Foreback, B., Bäck, J., Petäjä, T., Makkonen, R., Kerminen, V.-M., Pihlatie, M., Aalto, J., & Kulmala, M. (2022). Positive feedback mechanism between biogenic volatile organic compounds and the methane lifetime in future climates. *npj Climate and Atmospheric Science*, *5*(1). https://doi.org/10.1038/s41612-022-00292-0

Gagan, S., Sarang, K., Rudzinski, K. J., Liu, R., Szmigielski, R., & Zhang, Y. (2023). Synthetic strategies for oxidation products from biogenic volatile organic compounds in the atmosphere: A review. *Atmospheric Environment*, *312*. https://doi.org/10.1016/j.atmosenv.2023.120017

Grote, R., Sharma, M., Ghirardo, A., & Schnitzler, J.-P. (2019). A new modeling approach for estimating abiotic and biotic stress-induced de novo emissions of biogenic volatile organic compounds from plants. *Frontiers in Forests and Global Change*, *2*. https://doi.org/10.3389/ffgc.2019.00026

Guenther, A., Jiang, X., Heald, C., Sakulyanontvittaya, T., Duhl, T., Emmons, L., & Wang, X. (2012). The model of emissions of gases and aerosols from nature version 2.1 (megan2.1): An extended and updated framework for modeling biogenic emissions. *Geoscientific Model Development*, (6). https://doi.org/10.5194/gmd-5-1471-2012

Hari, P., & Kulmala, M. (2005). Station for measuring ecosystem-atmosphere relations (smear ii). *BOREAL ENVIRONMENT RESEARCH*, *10*(5), 315–322.

Hinds, W. C. (1999). *Aerosol technology : Properties, behavior, and measurement of airborne particles.* Wiley.

IPCC. (2021). Summary for policymakers. In V. Masson-Delmotte, P. Zhai, A. Pirani, S. Connors, C. Péan, S. Berger, N. Caud, Y. Chen, L. Goldfarb, M. Gomis, M. Huang, K. Leitzell, E. Lonnoy, J. Matthews, T. Maycock, T. Waterfield, O. Yelekçi, R. Yu, & B. Zhou (Eds.), *Climate change 2021: The physical science basis. contribution of working group i to the sixth assessment report of the intergovernmental panel on climate change* (332). Cambridge University Press. https://doi.org/10.1017/9781009157896.001

Jaakkola, E. (2024). Stress-induced bvoc emissions from forests in sweden. *MERGE: ModElling the Regional and Global Earth system BECC: Biodiversity and Ecosystem services in a Changing Climate.*

Jimenez, J. L., Canagaratna, M. R., Donahue, N. M., Prevot, A. S. H., Zhang, Q., Kroll, J. H., DeCarlo, P. F., Allan, J. D., Coe, H., Ng, N. L., Aiken, A. C., Docherty, K. S., Ulbrich, I. M., Grieshop, A. P., Robinson, A. L., Duplissy, J., Smith, J. D., Wilson, K. R., Lanz, V. A., ... Trimborn, A. (2009). Evolution of organic aerosols in the atmosphere. *Science*, *326*(5959), 1525–1529. https://doi.org/10.1126/science.1179518

Junninen, H., Lauri, A., Keronen, P., Aalto, P., Hiltunen, V., Hari, P., & Kulmala, M. (2009). Smart-smear: On-line data exploration and visualization tool for smear stations. *Boreal Environment Research*, *14*, 447–457.

Krikken, F., van Oldenborgh, G., Lehner, F., Haustein, K., & Drobyshev, I. (2021). Attribution of the role of climate change in the forest fires in sweden 2018. *Natural Hazards and Earth System Sciences*, *21*(7), 2169-2179 –2179. https://doi.org/10.5194/nhess-21-2169-2021

Kulmala, M., Pohja, T., Hakola, H., Kajos, M. K., Rinne, J., Ruuskanen, T. M., & Taipale, R. (2008). Technical note: Quantitative long-term measurements of voc concentrations by ptr-ms measurement, calibration, and volume mixing ratio calculation methods. *Atmospheric Chemistry and Physics*, *8*(22), 6681–6698. www.atmos-chem-phys.net/8/6681/2008/

Kulmala, M., Rinne, J., Petäjä, T., Maso, M. D., Patokoski, J., Manninen, H. E., Hõrrak, U., Asmi, E., Aalto, P. P., Hirsikko, A., Yli-Juuti, T., Nieminen, T., & Riipinen, I. (2011). Growth rates of nucleation mode particles in hyytiälä during 20032009: Variation with particle size, season, data analysis method and ambient conditions. *Atmospheric Chemistry and Physics*, *11*(24), 12865–12886. https://doi.org/10.5194/acp-11-12865-2011

Kumala, M., & Petäjä, T. (2024). Particle number size distribution - dmps at hyytiälä, data hosted by ebas at nilu [University of Helsinki, Institute for Atmospheric and Earth System Research].

Lehtonen, I., & Venäläinen, A. (2021). The exceptional nordic forest fire season 2018 in the context of climate change. *FMI's Climate Bulletin: Research Letters*, *3*(1), 8–10. https://doi.org/10.35614/ISSN-2341-6408-IK-2021-03-RL

Mahilang, M., Deb, M. K., & Pervez, S. (2021). Biogenic secondary organic aerosols: A review on formation mechanism, analytical challenges and environmental impacts. *CHEMOSPHERE*, *262*, 127771. https://doi.org/10.1016/j.chemosphere.2020.127771

Olenius, T., & Roldin, P. (2022). Role of gas–molecular cluster–aerosol dynamics in atmospheric new-particle formation. *Scientific Reports*, *12*(1). https://doi.org/10.1038/s41598-022-14525-y

Otu-Larbi, F., Wild, O., Ashworth, K., Bolas, C., Staniaszek, Z., Jones, R., Ferracci, V., Harris, N., & Malhi, Y. (2020). Modelling the effect of the 2018 summer heatwave and drought on isoprene emissions in a uk woodland. *Global Change Biology*, *26*(4), 2320-2335 –2335. https://doi.org/10.1111/gcb.14963

Roldin, P., Ehn, M., Kurtén, T., Olenius, T., Rissanen, M. P., Sarnela, N., Elm, J., Rantala, P., Hao, L., Hyttinen, N., Heikkinen, L., Worsnop, D. R., Pichelstorfer, L., Xavier, C., Clusius, P., Öström, E., Petäjä, T., Kulmala, M., Vehkamäki, H., ... Boy, M. (2019). The role of highly oxygenated organic molecules in the boreal aerosol-cloud-climate system. *Nature Communications MERGE: ModElling the Regional and Global Earth system*, *10*, 1–15. https://doi.org/10.1038/s41467-019-12338-8

Roldin, P., Swietlicki, E., Schurgers, G., Arneth, A., Lehtinen, K. E. J., Boy, M., & Kulmala, M. (2011). Development and evaluation of the aerosol dynamics and gas phase chemistry model adchem. *Atmospheric Chemistry and Physics NanoLund: Center for Nanoscience MERGE: ModElling the Regional and Global Earth system*, *11*(12), 5867–5896. https://doi.org/10.5194/acp-11-5867-2011

Schurgers, G., Arneth, A., Holzinger, R., & Goldstein, A. H. (2009). Process-based modelling of biogenic monoterpene emissions combining production and release from storage. *Atmospheric Chemistry and Physics*, *9*(10), 3409–3423. www.atmos-chem-phys.net/9/3409/2009/

Shan-Hu, L., Gordon, H., Huan, Y., Lehtipalo, K., Haley, R., Yixin, L., & Renyi, Z. (2019). New particle formation in the atmosphere: From molecular clusters to global climate. *Journal of Geophysical Research: Atmospheres*, *124*(13), 7098–7146. https://doi.org/10.1029/2018JD029356

Šimpraga, M., Ghimire, R. P., Van Der Straeten, D., Blande, J. D., Kasurinen, A., Sorvari, J., Holopainen, T., Adriaenssens, S., Holopainen, J. K., & Kivimäenpää, M. (2019). Unravelling the functions of biogenic volatiles in boreal and temperate forest ecosystems. *European Journal of Forest Research*, *138*(5), 763–787. https://doi.org/10.1007/s10342-019-01213-2

Sinclair, V. A., Mikkola, J., Rantanen, M., & Räisänen, J. (2019). The summer 2018 heatwave in finland. *Weather*, *74*(11), 403–409. https://doi.org/10.1002/wea.3525

Sindelarova, K., Markova, J., Simpson, 1., David, Huszar, P., Karlicky, J., Darras, S., & Granier, C. (2022). High-resolution biogenic global emission inventory for the time period 2000-2019 for

air quality modelling. *Earth System Science Data*, *14*(1), 251–270. https://doi.org/10.5194/essd-14-251-2022

Smith, B., Prentice, I. C., & Sykes, M. T. (2001). Representation of vegetation dynamics in the modelling of terrestrial ecosystems: Comparing two contrasting approaches within european climate space. *Global Ecology and Biogeography*, *10*(6), 621–637.

Weber, J., Archer-Nicholls, S., Abraham, N. L., Shin, Y. M., Griffiths, P., Grosvenor, D. P., Scott, C. E., & Archibald, A. T. (2022). Chemistry-driven changes strongly influence climate forcing from vegetation emissions. *Nature Communications*, *13*(1), 1–12. https://doi.org/10.1038/s41467-022-34944-9

Wilcke, R. A. I., Kjellström, E., Lin, C., Matei, D., Moberg, A., & Tyrlis, E. (2020). The extremely warm summer of 2018 in sweden - set in a historical context. *Earth System Dynamics*, *11*(4), 1107–1121. https://doi.org/10.5194/esd-11-1107-2020

Xavier, C., de jonge, R. W., Jokinen, T., Beck, L., Sipilä, M., Olenius, T., & Roldin, P. (2024). Role of iodine-assisted aerosol particle formation in antarctica. *Environmental Science & Technology*, *58*(17), 7314–7324. https://doi.org/10.1021/acs.est.3c09103

Xue, C., Krysztofiak, G., Ren, Y., Cai, M., Mercier, P., Fur, F. L., Robin, C., Grosselin, B., Dae¨le, V., Mcgillen, M. R., Mu, Y., Catoire, V., & Mellouki, A. (2024). A study on wildfire impacts on greenhouse gas emissions and regional air quality in south of orle´ans, france. *Journal of Environmental Sciences*, 521–533. https://doi.org/10.1016/j.jes.2022.08.032

Yli-Juuti, T., Isokääntä, S., Mikkonen, S., Nieminen, T., Virtanen, A., Mielonen, T., Arola, A., Laakso, A., Lipponen, A., Romakkaniemi, S., Tonttila, J., Kokkola, H., Heikkinen, L., Ehn, M., Keskinen, H.-M., Kulmala, M., Luoma, K., Paasonen, P., & Petäjä, T. (2021). Significance of the organic aerosol driven climate feedback in the boreal area. *Nature Communications*, *12*(1). https://doi.org/10.1038/s41467-021-25850-7

Appendix A

Appendix A provides figures referenced in the section 4.1.

BVOC Emission Maps

The following maps present the emission anomalies in 2018 and 2017 compared to a reference period (2003-2016).

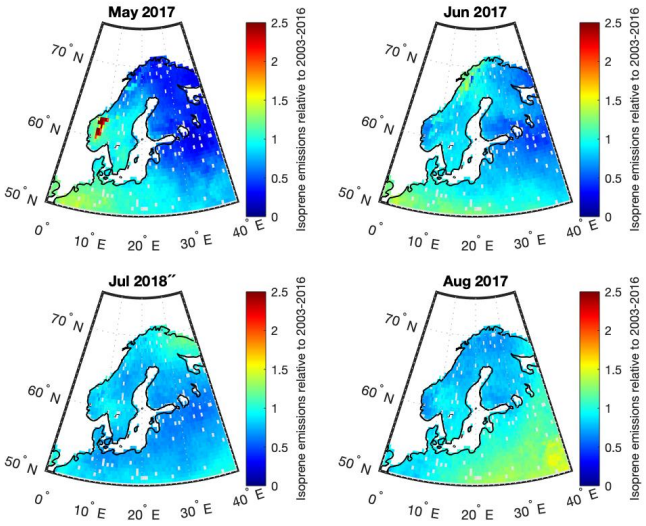

Figure 19: Average monthly isoprene emissions for 2017, divided by average isoprene emissions for the respective month 2003-2016 (from LPJ-GUESS)

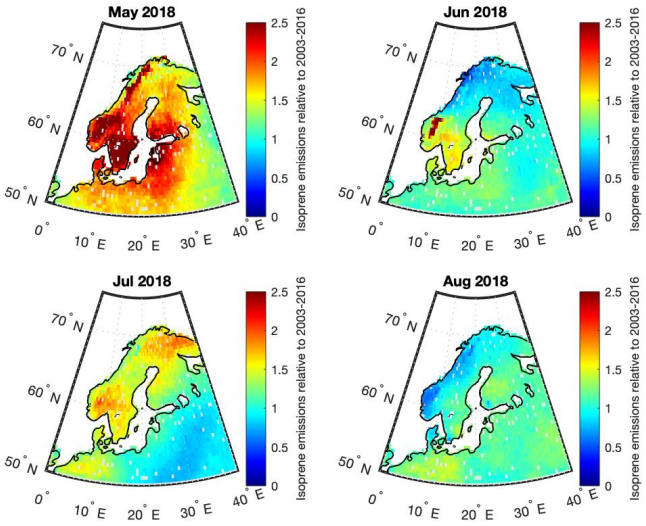

Figure 20: Average monthly isoprene emissions for 2018, divided by average isoprene emissions for the respective month 2003-2016 (from LPJ-GUESS)

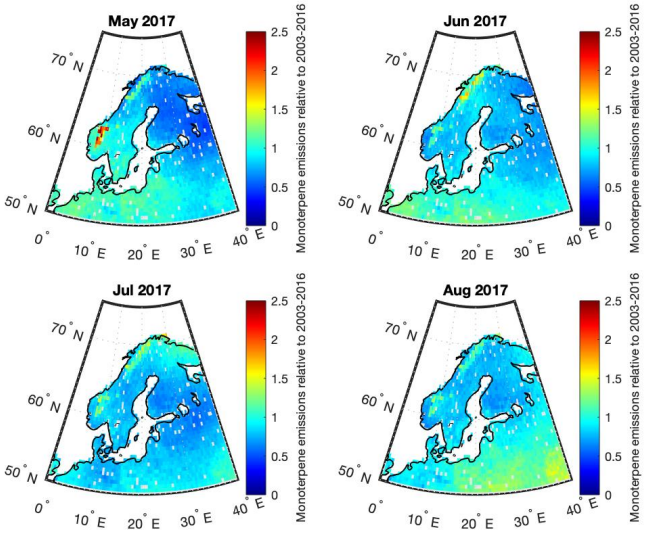

Figure 21: Average monthly monoterpene emissions for 2017, divided by average monoterpene emissions for the respective month 2003-2016 (from LPJ-GUESS)

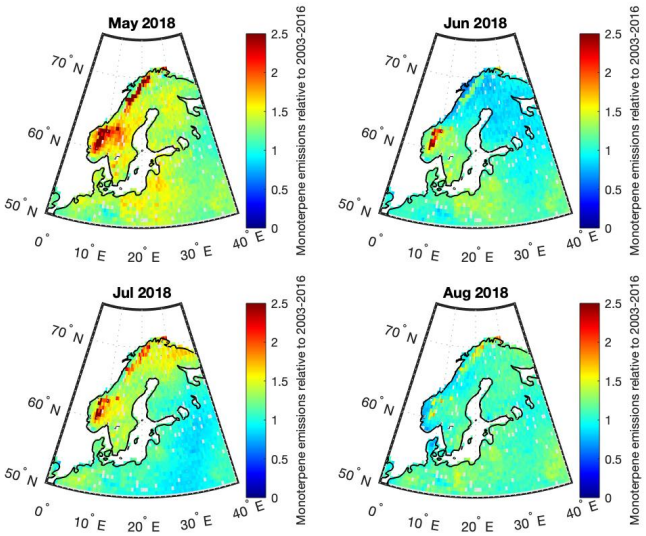

Figure 22: Average monthly monoterpene emissions for 2018, divided by average monoterpene emissions for the respective month 2003-2016 (from LPJ-GUESS)

BVOC Emissions from CAMS Compared with BVOC Emisisons from LPJ-GUESS

The below figures show emissions of isoprene, total monoterpenes and α-pinene from CAMS plotted against the respective emissions from LPJ-GUESS.

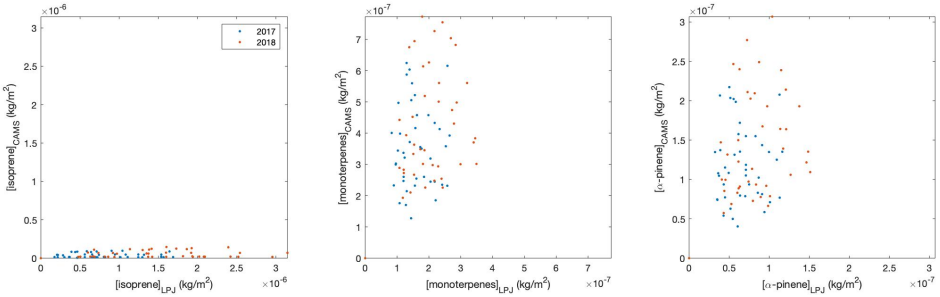

Figure 23: Cumulative emissions from LPJ-GUESS along HYSPLIT airmass trajectories plotted against cumulative emissions from CAMS, starting 3 h from the Hyytiälä measurement station (May 2018 and 2017)

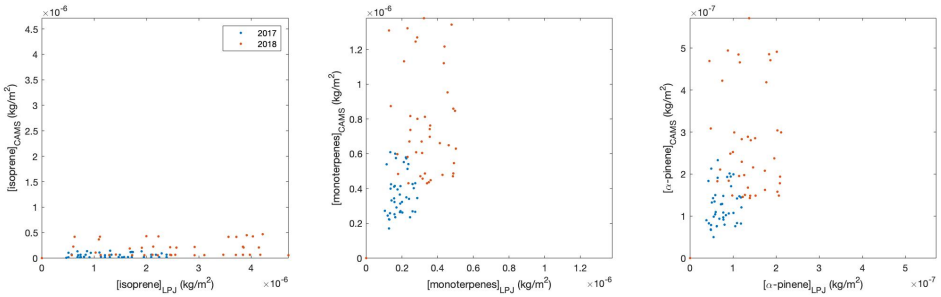

Figure 24: Cumulative emissions from LPJ-GUESS along HYSPLIT airmass trajectories plotted against cumulative emissions from CAMS, starting 3 h from the Hyytiälä measurement station (June 2018 and 2017)

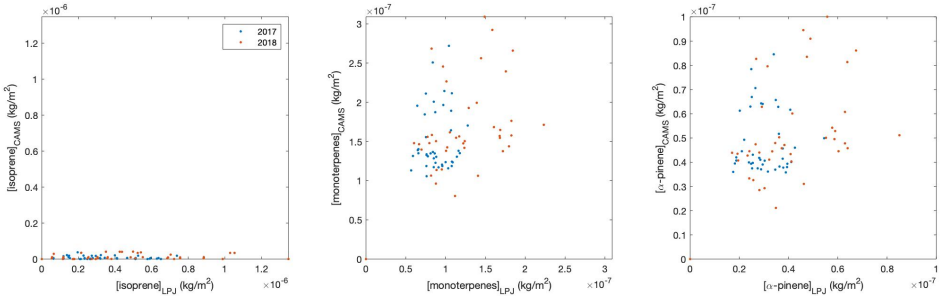

Figure 25: Cumulative emissions from LPJ-GUESS along HYSPLIT airmass trajectories plotted against cumulative emissions from CAMS, starting 3 h from the Hyytiälä measurement station (August 2018 and 2017)

Appendix B

Appendix B provides the figures and tables referenced in section 4.2 in the report.

Comparison between Modelled and Measured BVOC Concentrations

Table 3: The table show the modelled median isoprene and monoterpene concentration (for setups using CAMS emissions) for each month as a factor of the meadured median concentration for the respective compound and month.

Compound	Model setup	Factor of Measured Median			
		May	June	July	August
Isoprene	CAMS 2017	2.05	1.36	0.79	0.62
	CAMS 2018	2.04	0.63	0.80	0.81
	CAMSx2	2.42	0.69	1.16	1.20
Monoterpenes	CAMS 2017	0.69	0.50	0.37	0.30
	CAMS 2018	0.60	0.42	0.41	0.38
	CAMSx2	1.90	1.26	1.48	1.19

Table 4: The table show the modelled median isoprene and monoterpene concentration (for setups using LPJ-GUESS emissions) for each month as a factor of the meadured median concentration for the respective compound and month.

Compound	Model setup	Factor of Measured Median			
		May	June	July	August
Isoprene	LPJ 2017	36.7	37.5	24.4	24.3
	LPJ 2018	37.6	22.2	15.8	22.2
Monoterpenes	LPJ 2017	0.43	0.28	0.26	0.19
	LPJ 2018	0.41	0.27	0.25	0.26

Particle Volume and Number, and Comparison Between Model Setups

Table 5: The table presents the relative change in particle number (PN) and particle volume (PV) between 2017 and 2018 for the LPJ and CAMS model setups, as well as the measured PN and PV.

	LPJ 2018 / LPJ 2018				CAMS 2018 / CAMS 2017				Measured 2017/ 2018			
	M	J	J	A	M	J	J	A	M	J	J	A
PN	1.04	1.02	0.81	1.06	0.97	1.02	0.79	1.03	1.58	1.37	1.32	1.39
PV	2.04	1.04	1.26	0.91	2.22	0.95	1.00	1.25	1.91	1.00	2.9	0.99

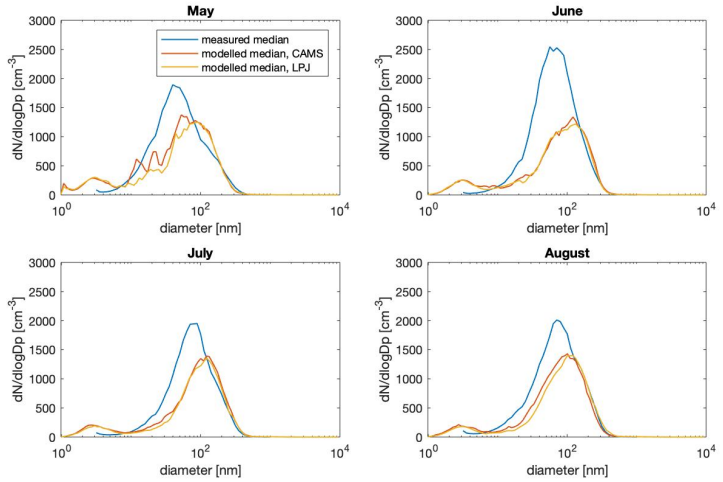

Figure 26: Comparison between modelled and measured median particle number size distribution at Hyytiälä, 2017 (summer months, MJJA).

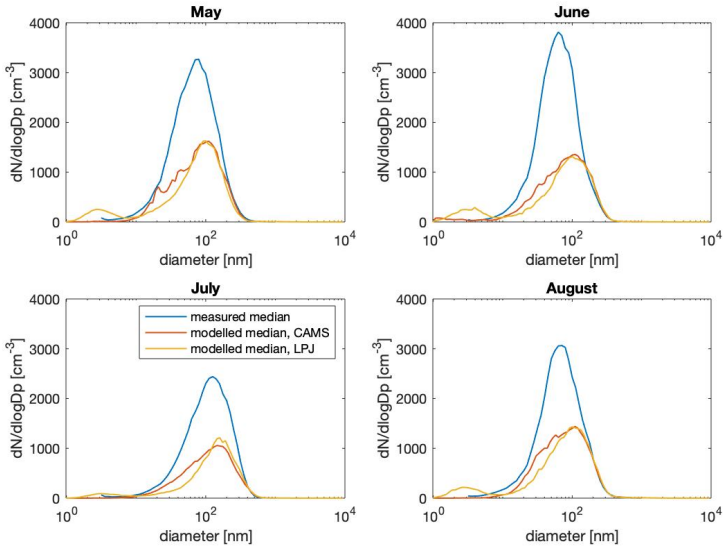

Figure 27: Comparison between modelled and measured median particle number size distribution at Hyytiälä, 2018 (summer months, MJJA).

Timeseries, LPJ

The following figures include the modelled concentrations of isoprene, monoterpenes, O_3, NO_2, NO, OH and NO_3 for model setups LPJ 2017 and 2018.

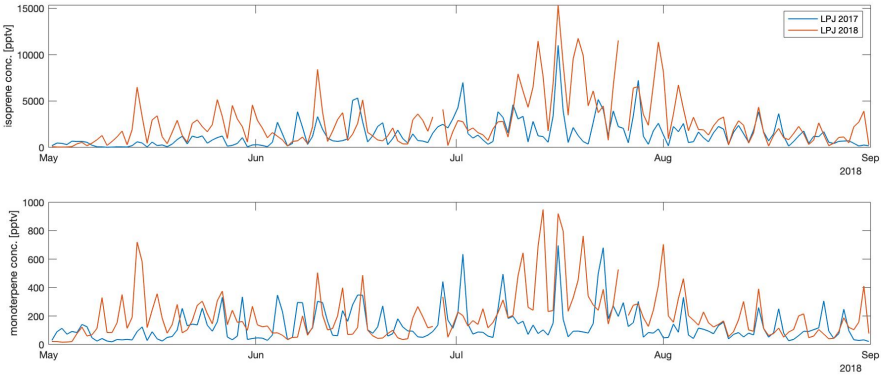

Figure 28: Modelled isoprene and monoterpene concentration for May - August 2018 in Hyytiälä for model setups LPJ 2017 and 2018 in ADCHEM

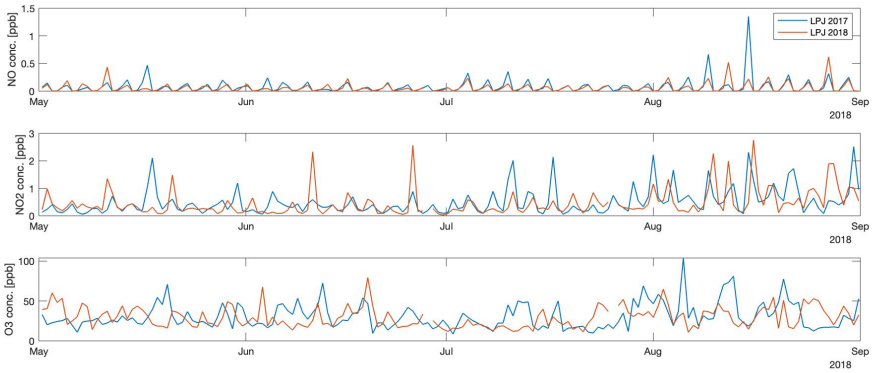

Figure 29: Modelled NO, NO2 and O3 concentration for May - August 2018 in Hyytiälä for model setups LPJ 2017 and 2018 in ADCHEM

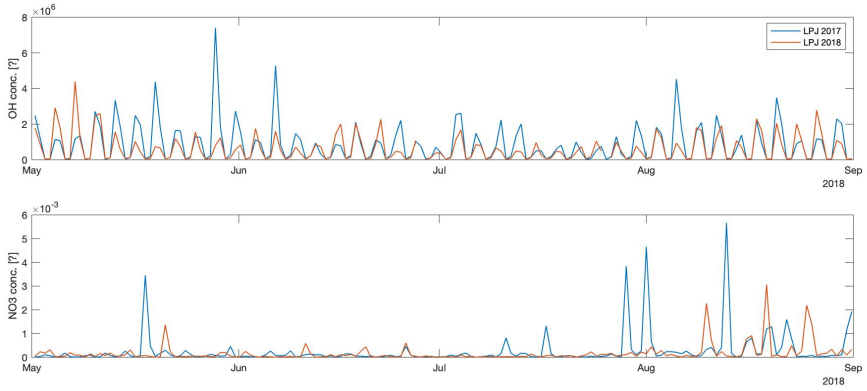

Figure 30: Modelled NO3 and OH concentration for May - August 2018 in Hyytiälä for model setups LPJ 2017 and 2018 in ADCHEM

Timeseries, CAMS

The following figures include the modelled concentrations of isoprene, monoterpenes, O_3, NO_2, NO, OH and NO_3 for model setups CAMS 2017 and 2018.

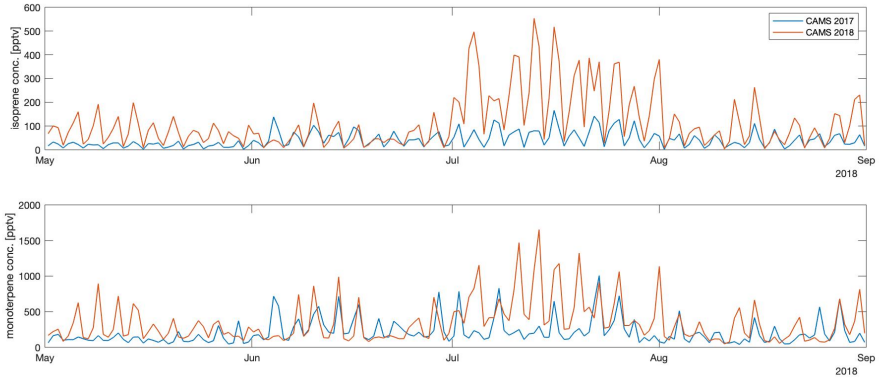

Figure 31: Modelled isoprene and monoterpene concentration for May - August 2018 in Hyytiälä for model setups CAMS 2017 and 2018 in ADCHEM

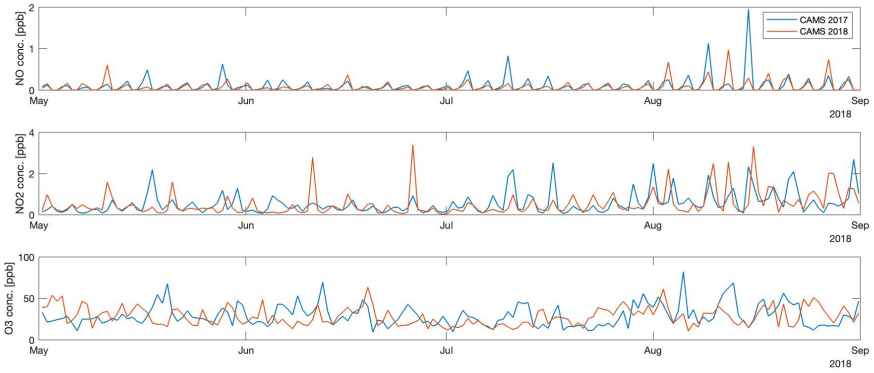

Figure 32: Modelled NO2, NO and O3 concentration for May - August 2018 in Hyytiälä for model setups CAMS 2017 and 2018 in ADCHEM

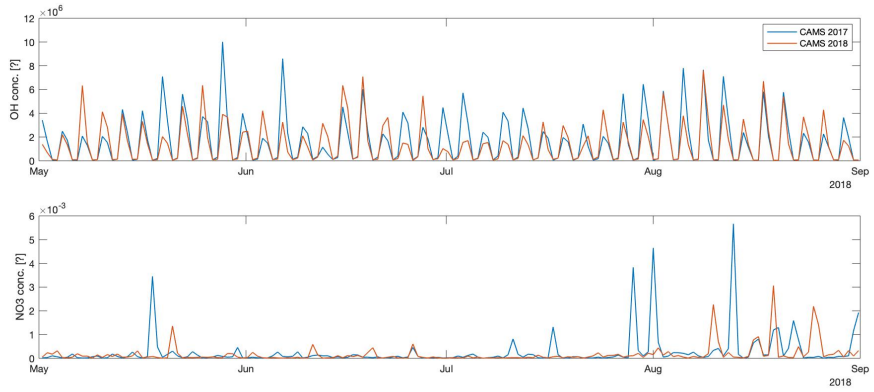

Figure 33: Modelled NO3 and OH concentration for May - August 2018 in Hyytiälä for model setups CAMS 2017 and 2018 in ADCHEM

Appendix C

Appendix C includes the figures and tables referenced in section 4.2.1 in the report.

Table 6: The table presents the relative change in particle number (PN) and particle volume (PV) between the CAMS 2018 and CAMSx2 model setups.

	CAMSx2 / CAMS 2018			
	M	J	J	A
PN	0.95	0.98	1.01	0.80
PV	1.21	1.22	2.03	1.14

Timeseries, CAMSx2

The following figures include the modelled concentrations of isoprene, monoterpenes, O_3, NO_2, NO, OH and NO_3 for model setups CAMS 2018 and CAMSx2 2018.

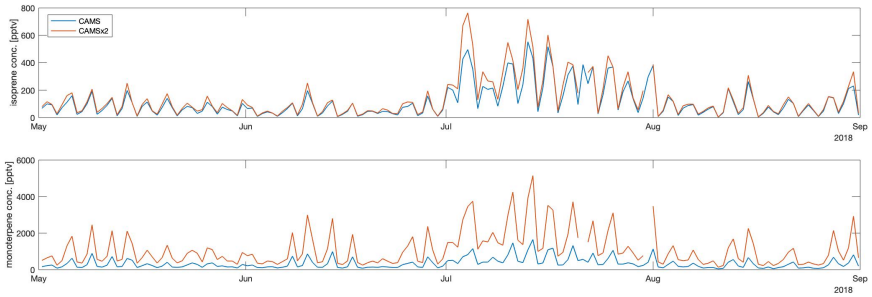

Figure 34: Modelled BVOC concentration for May - August 2018 in Hyytiälä for model setups CAMS and CAMSx2 in ADCHEM

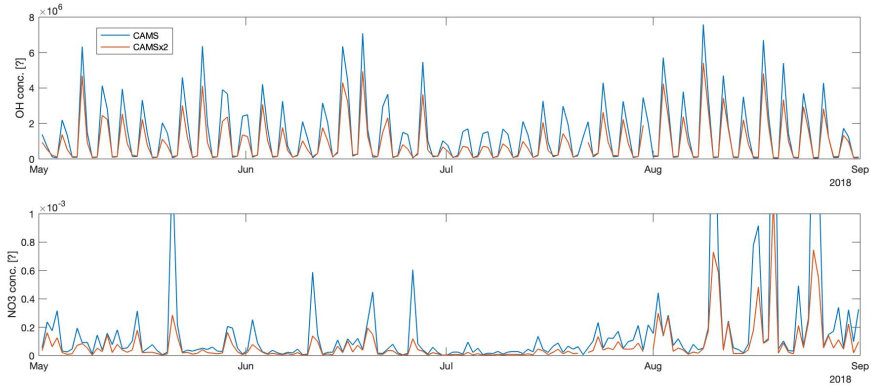

Figure 35: Modelled NO3 and OH concentration for May - August 2018 in Hyytiälä for model setups CAMS and CAMSx2 in ADCHEM. (Note that the NO3 graph is cut off at 1e-3 as to better see the difference at lower concentrations).

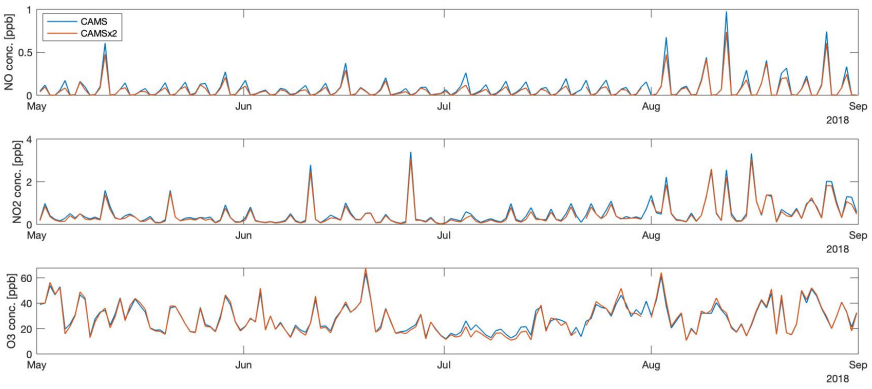

Figure 36: Modelled NO, NO2 and O3 concentration for May - August 2018 in Hyytiälä for model setups CAMS and CAMSx2 in ADCHEM